LIBRARY
RESEARCH REPORTS DIVISION
NAVAL POSTGRADUATE SCHOOL
MONTEREY, CALIFORNIA 93943
ADA800396

RETENTION COPY

PRESSURE DISTRIBUTIONS OVER BODIES OF REVOLUTION FOR AXIAL FLOW

(DRUCKVERTEILUNGEN VON ROTATIONSKORPERN BEI ACHSIALER ANSTROMUNG)

by

M. Brand

Aerodynamische Versuchsanstalt Göttingen e. V.
UM Nr. 3206, 30 December 1944

Translated by C.J. Wenzinger

ADVANCE COPY

To make the information contained in this translation immediately available to those who need it most urgently, a small number of copies of the unedited first draft have been printed. Recipients will be requested to return their advance copies on issuance of the final edition.

Navy Department
David Taylor Model Basin,
Washington, D.C.

April 1947

Translation 220

LIBRARY
DAVID W. TAYLOR MODEL BASIN
NAVY DEPARTMENT

Pressure Distributions over Bodies of Revolution for Axial Flow.

Abstract: Calculated pressure distributions are given in the following report for 12 half-bodies and for 59 bodies of revolution for the case of axial flow. The nose radius, the thickness distribution, and the trailing-edge angle were varied, while the fineness ratio was assumed practically constant throughout at 1:5. After a review of the systematic calculations, examples are given for bodies with assigned contours, as well as a discussion of the effects of other fineness ratios on the pressure distribution.

Outline:

I. Designations of the Body of Revolution
II. Review of the Calculated Bodies of Revolution.
III. Bodies of Revolution with Assigned Contours.
IV. Discussion.
V. References.

I. Designations of the Body of Revolution.

An account is given in the following report of 59 bodies of revolution and 12 half-bodies with their calculated pressure distributions for the case of axial flow. The calculations were based on the method of singularities, as presented by F. Riegels and W. Brand in UM* Report 3106. A review is given on page 11 of the singularity distributions used, and the constants used in the calculations are listed on pages 12 through 14.

First of all the review deals with the separate singularity elements that are used to produce the bodies of revolution, which

* See the reference on page 7.

elements as sources produce half bodies in a parallel flow. The length of a singularity element is designated by x_o, the infinite asymptotically-attained boundary radius of the half body by R_o, ($2R_o = D_\infty$). The ratio of the strength E of the singularity element to the velocity of oncoming flow determines the value of this boundary radius, ($E/\pi v_o = R_o^2$). The summary on page 12 therefore presents this ratio, and in such a manner, that the values of the boundary radius R_o are referred to the lengths x_o of the singularity elements, (R_o^2/x_o^2). An area of 1 cm^2 signifies thereby a value of $R_o^2/x_o^2 = 0.20$ in the summary of half bodies on page 11.

The summary on page 11 also gives the combined singularity distributions of bodies of revolution from the separate singularity elements. Each distribution is thereby designated according to the plan:

(1) The series number -
For example, V3 is the third model of the fifth series

(2) The short designation of the body -
For example, 0.46 - 20 - 40
The first number indicates the nose radius ($\rho / l / d^2_{max} / l^2$), where ρ is the nose radius, l is the length, and d_{max} is the maximum diameter of the body;
the second number is the maximum diameter of the body in percent of its length; and
the third number is the rearward position of the maximum thickness in percent of the length of the body.

The summary on pages 12-14 contains the following data for the

calculated bodies of revolution and the half-bodies:

(1) The ratios of the separate source - (E_v) bzw. sink strength (E'_v) to the total strength of all sources of a singularity combination.

(2) The ratios of the total strength of all sources of a combination (E) to the velocity of oncoming flow, in the form R_o^2/L^2; ($R_o^2/L^2 = E/\pi v_o L^2$). The boundary radius R_o is in this case also referred to the distance L, which extends from the beginning of the first source element to the end of the last sink element. In the data presented on page 11, 1 cm^2 signifies $R_o^2/L^2 = 0.0512$.

(3) The length x_{o_v} of the source element, referred to the distance L.

(4) The length x'_{o_v} of the sink element, referred to the distance L.

It should be noted that, as concerns the data for the coordinates of the bodies of revolution, they were determined graphically and therefore have a limited accuracy.

II. Review of the Calculated Bodies of Revolution.

The pressure distributions of the closed bodies of revolution precede those of the half bodies, and in fact each three half bodies having different strength of the linearly-increasing, constant, linearly-decreasing and second-power decreasing source distances, were designated with their pressure distributions. The bodies of revolution then follow which are organized in eight series all of which have a fineness ratio d_{max}/l of about 1:5.

The first series contains four bodies which have the same nose radius but different thickness distributions and different

trailing-edge angles. Body I_1 is a source-sink body. The source point is maintained in the following three bodies but their sink points are displaced by a sink-distribution which is distributed further along the axis of each body.

The second series includes eight bodies in which the maximum thicknesses are located at about the 40 percent position and in which the trailing-edge angles are all about the same. Bodies are obtained with different nose radii by the choice of various source elements.

The third series, likewise with eight bodies, corresponds to the second series with exception of the rear portions of bodies III_7 and III_8, has the maximum thickness at 50 percent, and exhibits a variation in the nose radius similar to that of the second series. Body III_7 represents an ellipsoid of revolution and body III_8 possesses a constant pressure distribution to a good approximation.

The fourth series presents ten bodies of which the first six have their maximum thickness at 60 percent. Following these, however, the maximum thickness travels forward to the 45 percent position by the effect of the source strength which is concentrated more and more over the forward part. The trailing-edge angle is about the same for all of these bodies. The variations are due to the choice of different source elements which are all about 60 percent long. In this manner a wide variation of the nose radius is obtained. It is thus possible to obtain a good transition in pressure distribution from one which constantly decreases to the rear, to one which has a high suction peak at the front.

In the fifth series, eight bodies with almost equal thickness at the 60 percent location and about the same trailing-edge

angle, with the exception of V_8, have the source elements still further subdivided. The effect of this subdivision is investigated upon the resulting contours together with their pressure distributions.

The sixth series includes seven bodies based on the same type of singularity distribution, in which the separate singularity elements are chosen differently.

The seventh and eighth series with respectively four and eight bodies all have about the same forward parts, but for these cases a series of sink combinations were chosen.

III. Bodies of Revolution with Assigned Contours.

In order to complete these systematic calculations two examples are presented in which the contours are assigned. For this case the singularity distributions, given in a simplified manner in Report UM 3106, which in combination with a parallel flow produce the assigned bodies of revolution, must first be determined from the approximate equation $q(x') \sim r\, dr/dx'$. Figure 1 on page 8 gives a representation of them. The calculated points of the closed stream surface are shown in Figure 1B by crosses in addition to the previously-described contour. This stream surface is produced by the singularity distributions determined from the approximate equation. The good agreement attained is easily seen. Incidentally it should be noted that the "Teardrop" symmetrical body of revolution treated here, has been tested in the various high-speed wind tunnels for purposes of comparison.

IV. Discussion.

A comparison between the corresponding source-sink

distributions shows that bodies and pressure-distributions are evolved such that sudden transitions in the source-sink distributions are always associated with sharp changes of curvature in the contour and the accompanying excess velocities and high negative pressures. On the other hand such sudden changes in the source-sink distributions are not obtained up to the present time from certain definite measurements of the changes of curvature. It is thus not possible to produce all arbitrarily assigned bodies of revolution from such source-sink distributions along the axis, particularly those bodies in which sudden very sharp changes of curvature occur in the contour.

Since almost all of the assigned bodies of revolution have the same fineness ratio $d_{max}/l = 1:5$, some further comments may be made as to what extent the assigned pressure distributions may serve as a definite basis for pressure distributions of bodies of revolution of different fineness ratio. These bodies are assumed to have similar source-sink distributions for various total strengths of all of their sources or sinks. If the total strength is varied of all sources or sinks of a source-sink combination, there is obtained not the colinear distorted body of different fineness ratio, but a body which deviates only slightly from a colinear distorted one provided the strength variations are not too great. The pressure distributions are not distorted in a colinear manner either. It is therefore not possible to make exact statements regarding the transfer of the pressure distributions given in this report to bodies of different fineness ratios. The character of the pressure distribution may generally be maintained to a considerable extent, however, by variation of the total strength and similar source-sink distribution. Three bodies with different fineness ratios, namely 1:5,

1:7.8, and 1:10 were calculated using the source-sink distribution V_2. These bodies are presented in Figure 2 on page 9, together with their pressure distributions. In order to obtain a definite basis upon which the assigned pressure distributions can be extrapolated to other fineness ratios, the absolute pressure minimum on the maximum diameter d_{max}/l of the body of revolution is presented in Figure 3 for this example. Figure 4 shows the same type of plot for the half body in which the absolute pressure minimum is drawn along the boundary radius R_o/x_o.

V. References.

1. Georg Fuhrmann - Theoretische und experimentelle Untersuchungen an Ballonmodellen, Jahrb. der Motorluftschiff-Studiengesellsch. 1911/12

2. F. Riegels und M. Brand - Stromfunctionen und Geschwindigkeitsfelder räumlicher Quellstrecken und ihr handlicher Gebrauch zur Bestimmung von Umriss und Druckverteilung rotationssymmetrischer Körper mit Beispielen. UM 3106 (1944).

A

Source-sink distribution

Fuselage of the Russian pursuit Mig. 1

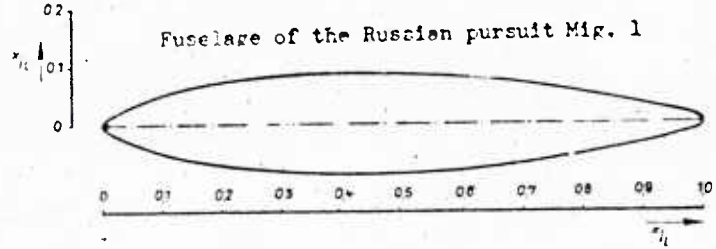

Pressure distribution

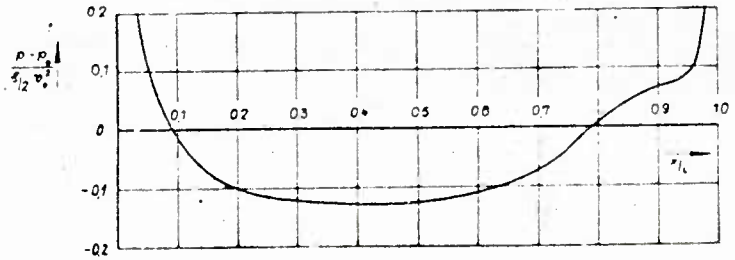

Figure 1

B

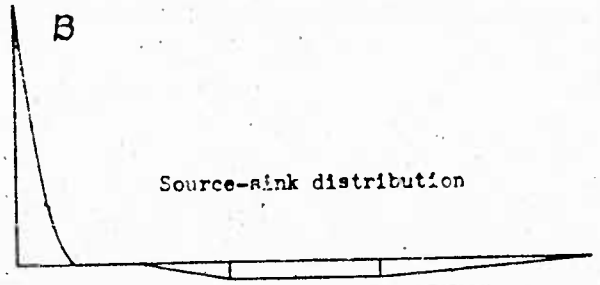

Source-sink distribution

Contour points produced by the assigned source-sink distribution in suitable parallel flow

Comparison Teardrop shape

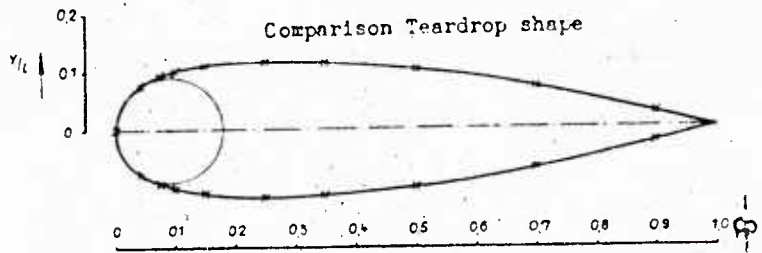

Pressure distribution

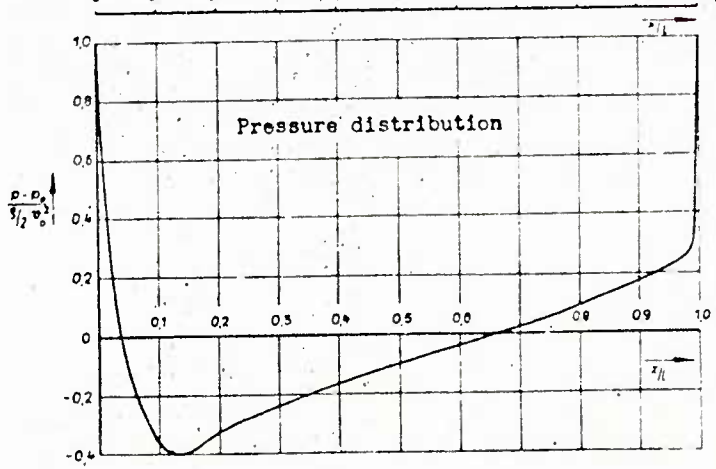

Bodies of revolution of the source-sink distribution V_1 with various total strengths of all sources

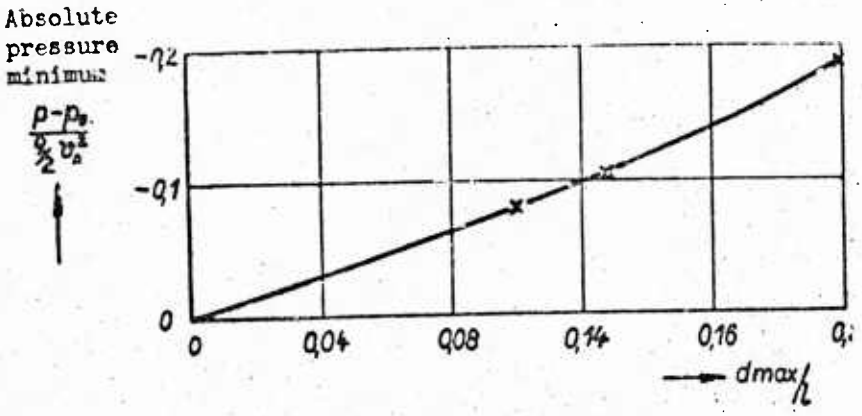

Figure 3

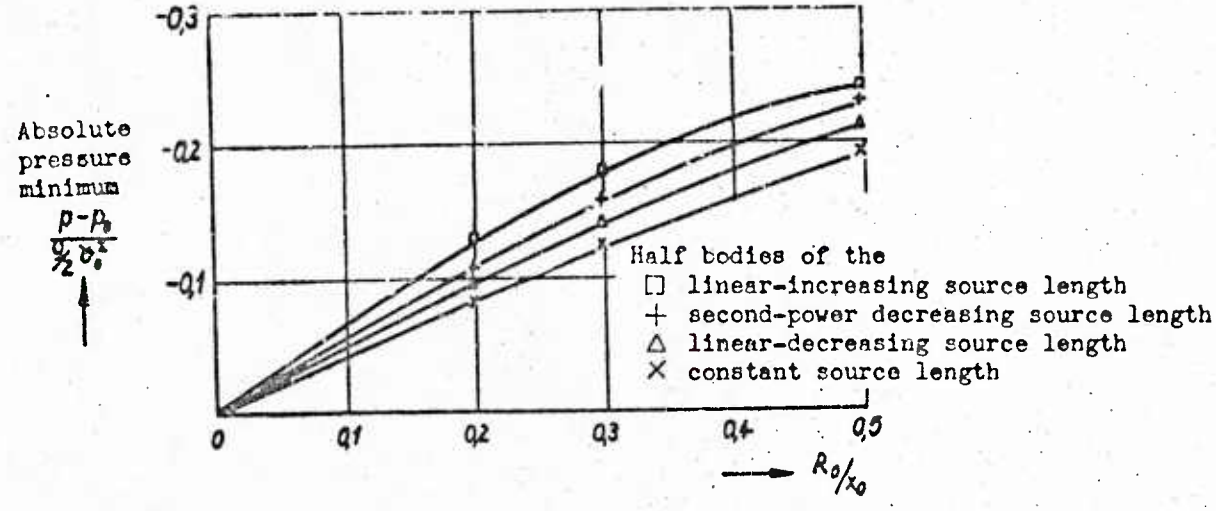

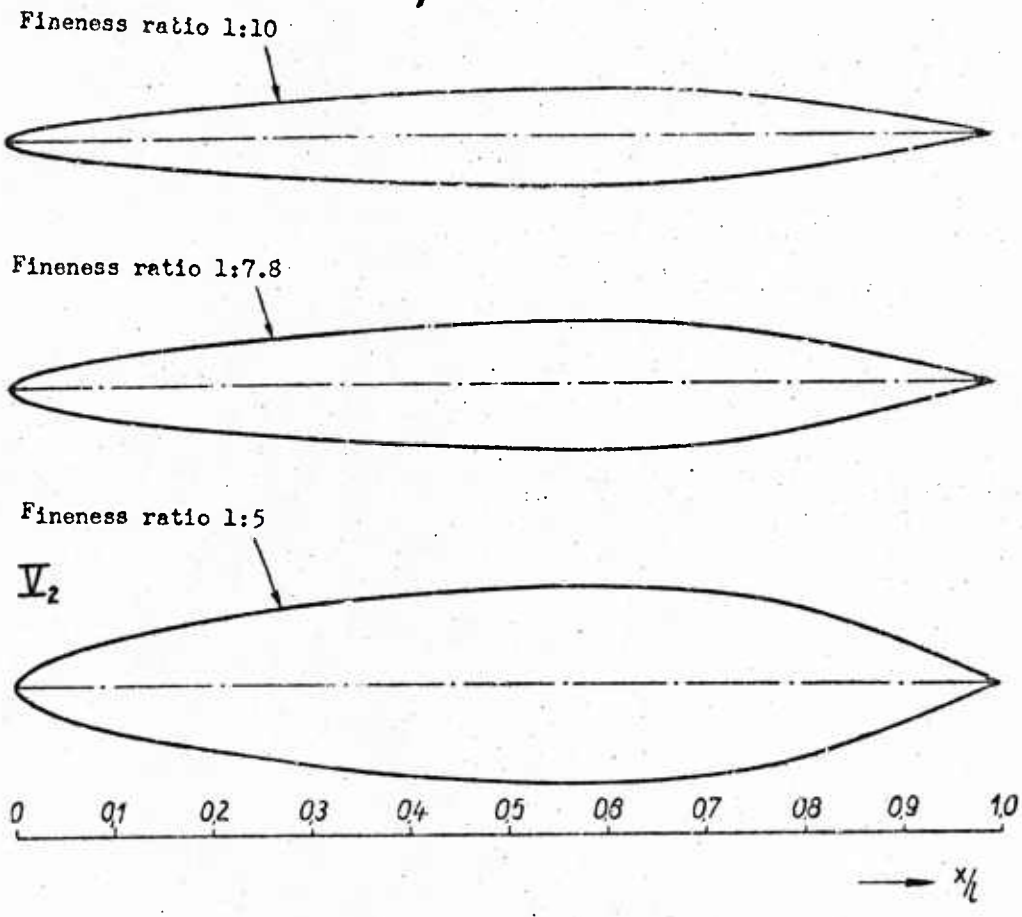
Fineness ratio 1:10
Fineness ratio 1:7.8
Fineness ratio 1:5
V_2
0
0,1
0,2
0,3
0,4
0,5
0,6
0,7
0,8
0,9
1,0
x/l

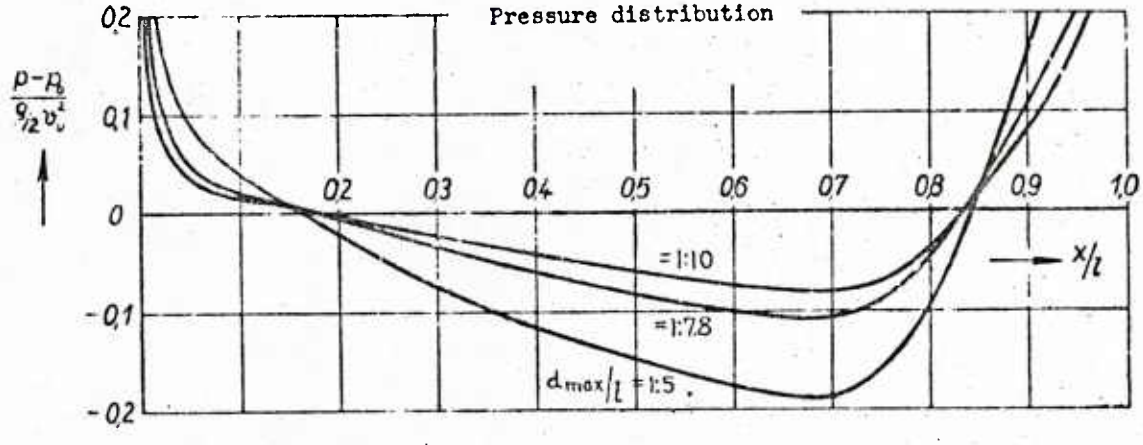
Pressure distribution
$\frac{p-p_0}{\rho/2 v_\infty^2}$
0,2
0,1
0
-0,1
-0,2
0,2
0,3
0,4
0,5
0,6
0,7
0,8
0,9
1,0
x/l
=1:10
=1:7.8
d_{max}/l = 1:5 .

Figure 2

Source elements of the half bodies

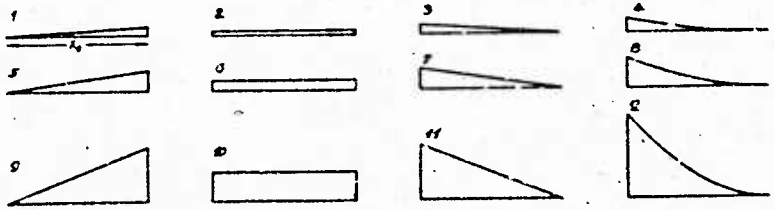

Source-sink distribution of the bodies of revolution

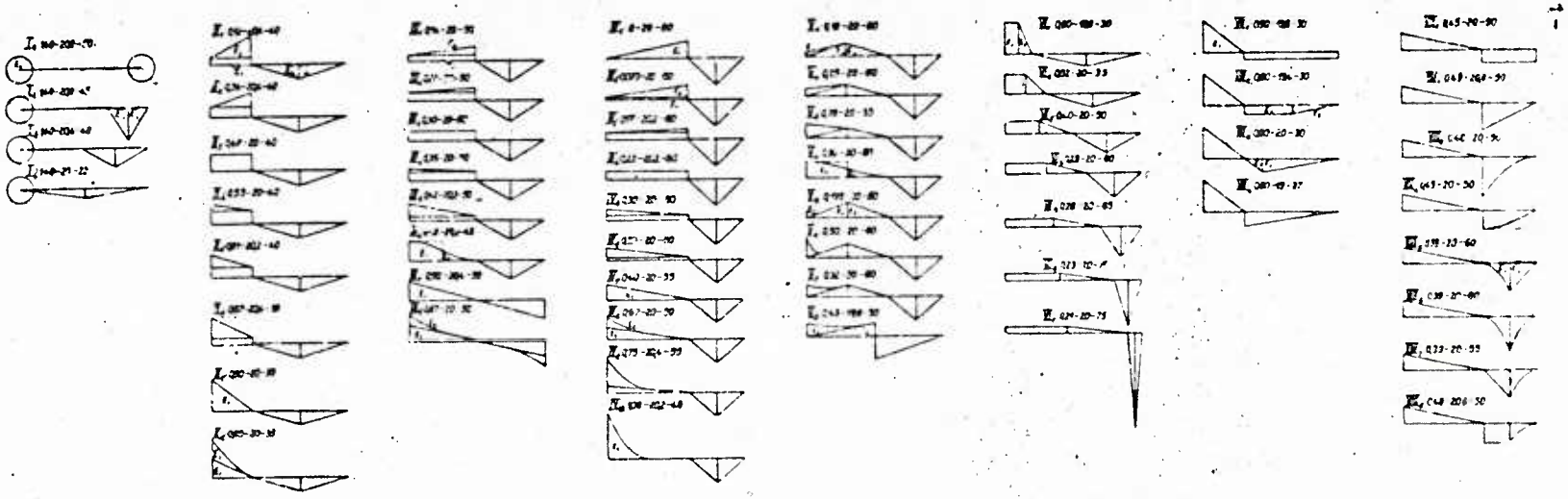

Half bodies	1	2	3	4	5	6	7	8	9
R_o^2/x_o^2	0,04	0,04	0,04	0,04	0,09	0,09	0,09	0,09	0,25
Half bodies	10	11	12						
R_o^2/x_o^2	0,25	0,25	0,25						

Bodies of revolution

Bez.	R_o^2/L^2	E_1/E	E_2/E	E_3/E	E_1'/E	E_2'/E	x_{o_1}/L	x_{o_2}/L	x_{o_3}/L	x'_{o_1}/L	x'_{o_2}/L
I_1	0,0142	1/1	-	-	1/1	-	-	-	-	-	-
I_2	0,0127	1/1	-	-	1/2	1/2	-	-	-	0,158	0,158
I_3	0,0127	1/1	-	-	1/2	1/2	-	-	-	0,263	0,263
I_4	0,0127	1/1	-	-	1/2	1/2	-	-	-	0,500	0,500
II_1	0,0125	2/5	3/5	-	1/2	1/2	0,3	0,3	-	0,35	0,35
II_2	0,0125	3/5	2/5	-	1/2	1/2	0,3	0,3	-	0,35	0,35
II_3	0,0120	1/1	-	-	1/2	1/2	0,3	0,3	-	0,35	0,35
II_4	0,0120	4/5	1/5	-	1/2	1/2	0,3	0,3	-	0,35	0,35
II_5	0,0120	3/5	2/5	-	1/2	1/2	0,3	0,3	-	0,35	0,35
II_6	0,0120	2/5	3/5	-	1/2	1/2	0,3	0,3	-	0,35	0,35
II_7	0,0115	1/1	-	-	1/2	1/2	0,3	0,3	-	0,35	0,35
II_8	0,0115	$\frac{1,3}{2,3}$	$\frac{1}{2,3}$	-	1/2	1/2	0,3	0,3	-	0,35	0,35
III_1	0,0125	3/5	2/5	-	1/2	1/2	0,5	0,5	-	0,25	0,25
III_2	0,0125	4/5	1/5	-	1/2	1/2	0,5	0,5	-	0,25	0,25
III_3	0,0120	1/1	-	-	1/2	1/2	0,5	0,5	-	0,25	0,25
III_4	0,0120	4/5	1/5	-	1/2	1/2	0,5	0,5	-	0,25	0,25
III_5	0,0120	2/5	3/5	-	1/2	1/2	0,5	0,5	-	0,25	0,25
III_6	0,0115	5/6	1/6	-	1/2	1/2	0,25	0,25	-	0,25	0,25
III_7	0,0120	1/1	-	-	1/1	-	0,5	-	-	0,5	-
III_8	0,0115	$\frac{3,6}{4,6}$	$\frac{1}{4,6}$	-	$\frac{3,6}{4,6}$	$\frac{1}{4,6}$	0,5	0,3	-	0,5	0,3
IV_1	0,0125	1/1	-	-	1/2	1/2	0,6	-	-	0,2	0,2
IV_2	0,0125	2/5	3/5	-	1/2	1/2	0,6	0,6	-	0,2	0,2
IV_3	0,0125	4/5	1/5	-	1/2	1/2	0,6	0,6	-	0,2	0,2
IV_4	0,0125	1/1	-	-	1/2	1/2	0,6	-	-	0,2	0,2

Bez.	R_o^2/L^2	E_1/E	E_2/E	E_3/E	E_1'/E	E_2'/E	x_{o_1}/L	x_{o_2}/L	x_{o_3}/L	x'_{o_1}/L	x'_{o_2}/L
IV_5	0,0120	$\frac{3}{4,8}$	$\frac{1,8}{4,8}$	-	1/2	1/2	0,6	0,6	-	0,2	0,2
IV_6	0,0115	$\frac{2}{4,6}$	$\frac{2,6}{4,6}$	-	1/2	1/2	0,6	0,6	-	0,2	0,2
IV_7	0,0115	1/1	-	-	1/2	1/2	0,6	-	-	0,2	0,2
IV_8	0,0115	$\frac{3,6}{4,6}$	$\frac{1}{4,6}$	-	1/2	1/2	0,6	0,3	-	0,2	0,2
IV_9	0,0115	$\frac{1,3}{2,3}$	$\frac{1}{2,3}$	-	1/2	1/2	0,6	0,3	-	0,2	0,2
IV_{10}	0,0110	1/1	-	-	1/2	1/2	0,3	-	-	0,2	0,2
V_1	0,01125	1/7	3/7	3/7	1/2	1/2	0,3	0,3	0,3	0,2	0,2
V_2	0,01125	1/4	$\frac{1,5}{4}$	$\frac{1,5}{4}$	1/2	1/2	0,3	0,3	0,3	0,2	0,2
V_3	0,01125	$\frac{1,5}{3,5}$	$\frac{1}{3,5}$	$\frac{1}{3,5}$	1/2	1/2	0,3	0,3	0,3	0,2	0,2
V_4	0,01125	5/6	1/6	-	1/2	1/2	0,3	0,3	-	0,2	0,2
V_5	0,01135	$\frac{1}{21}$	$\frac{10}{21}$	$\frac{10}{21}$	1/2	1/2	0,1	0,3	0,3	0,2	0,2
V_6	0,01135	1/7	3/7	3/7	1/2	1/2	0,1	0,3	0,3	0,2	0,2
V_7	0,01135	1/4	$\frac{1,5}{4}$	$\frac{1,5}{4}$	1/2	1/2	0,3	0,3	0,3	0,2	0,2
V_8	0,0132	$\frac{1}{2,5}$	$\frac{1,5}{2,5}$	-	1/1	-	0,5	0,5	-	0,5	-
VI_1	0,01125	2/3	1/3	-	1/2	1/2	0,1	0,1	-	0,4	0,4
VI_2	0,0115	2/3	1/3	-	1/2	1/2	0,15	0,15	-	0,35	0,35
VI_3	0,01125	2/3	1/3	-	1/2	1/2	0,25	0,25	-	0,25	0,25
VI_4	0,01125	2/3	1/3	-	1/2	1/2	0,3	0,3	-	0,2	0,2
VI_5	0,01125	2/3	1/3	-	1/2	1/2	0,35	0,35	-	0,15	0,15
VI_6	0,01125	2/3	1/3	-	1/2	1/2	0,4	0,4	-	0,1	0,1
VI_7	0,01125	2/3	1/3	-	1/2	1/2	0,45	0,45	-	0,05	0,05
VII_1	0,0115	1/1	-	-	1/1	-	0,3	-	-	0,7	-
VII_2	0,0115	1/1	-	-	2/3	1/3	0,3	-	-	0,35	0,35
VII_3	0,0115	1/1	-	-	$\frac{1,6}{7,3}$	$\frac{6}{7,3}$	0,3	-	-	0,135	0,565
VII_4	0,0115	1/1	-	-	1/1	-	0,3	-	-	0,7	-
$VIII_1$	0,01175	1/1	-	-	1/1	-	0,6	-	-	0,4	-
$VIII_2$	0,01277	1/1	-	-	1/1	-	0,6	-	-	0,4	-
$VIII_3$	0,0125	1/1	-	-	1/1	-	0,6	-	-	0,4	-
$VIII_4$	0,01175	1/1	-	-	1/1	-	0,6	-	-	0,4	-

Bez.	R_o^2/L^2	E_1/E	E_2/E	E_3/E	E'_1/E	E'_2/E	x_{o_1}/L	x_{o_2}/L	x_{o_3}/L	x'_{o_1}/L	x'_{o_2}/L
$VIII_5$	0,01125	1/1	-	-	2/5	3/5	0,6	-	-	0,2	0,2
$VIII_6$	0,01125	1/1	-	-	1/2	1/2	0,6	-	-	0,2	0,2
$VIII_7$	0,01125	1/1	-	-	2/5	3/5	0,6	-	-	0,2	0,2
$VIII_8$	0,0125	1/1	-	-	3/4	1/4	0,6	-	-	0,2	0,2

Bez.	R_o^2/L^2	E_1/E	E_2/E	E'_1/E	E'_2/E	E'_3/E	x_{o_1}/L	x_{o_2}/L	x'_{o_1}/L	x'_{o_2}/L	x'_{o_3}/L
A	0,00825	$\frac{3}{10}$	$\frac{7}{10}$	$\frac{4,1}{10}$	$\frac{2,8}{10}$	$\frac{3,1}{10}$	0,1	3,5	0,265	0,285	0,285
B	0,0159	1/1	-	$\frac{1,5}{10}$	$\frac{5}{10}$	$\frac{3,5}{10}$	0,1	-	0,19	0,25	0,35

1 Source length

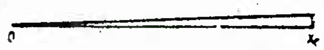

Half body of the linear source length with $R_o^2/X_o^2 = 0.04$

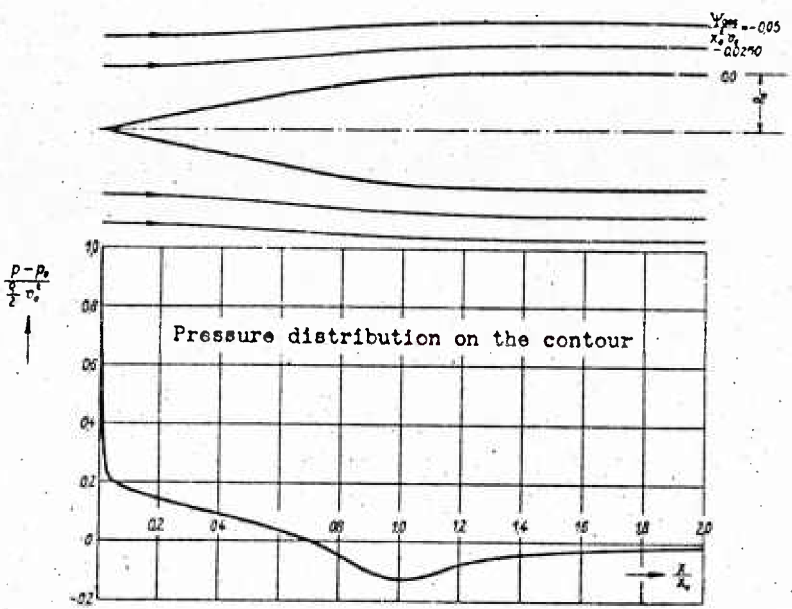

x/D	0	0,05	0,10	0,15	0,20	0,30	0,40	0,50	0,75	1,00	1,25	1,50	1,75	2,00	2,50	3,00	3,50	4,00	5,00
y/D	0	0,010	0,020	0,030	0,045	0,060	0,080	0,100	0,150	0,200	0,250	0,300	0,350	0,400	[illegible]	[illegible]	[illegible]	[illegible]	[illegible]

2 Source length

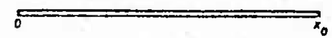

Half body of the constant source length with $R_o^2/X_o^2 = 0.04$

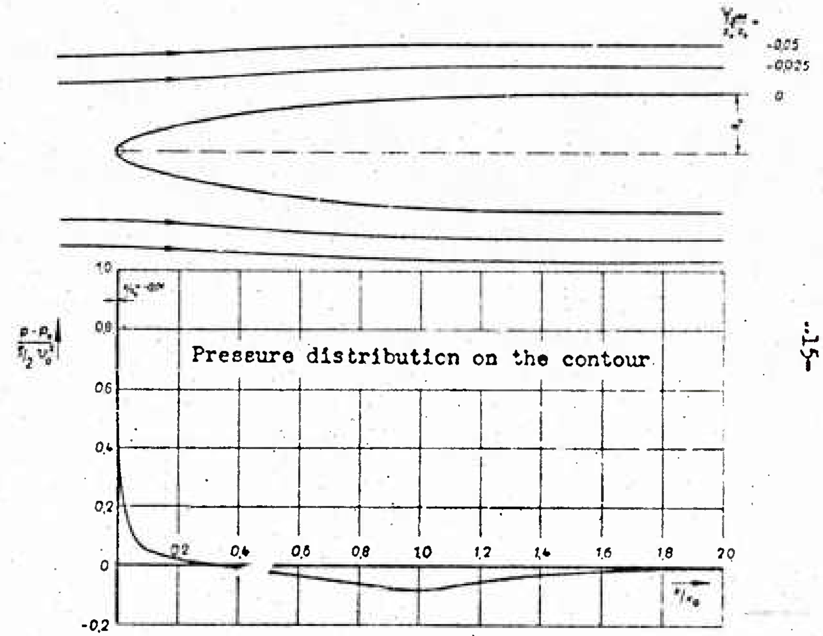

x/D_∞	0	0,05	0,10	0,15	0,20	0,30	0,40	0,50	0,75	1,00	1,25	1,50	1,75	2,00	2,50	3,00	3,50	4,00	5,00
y/D_∞	0	0,060	0,095	0,120	0,140	0,170	[illegible]	0,220	0,275	0,315	0,350	0,380	0,405	[illegible]	0,465	0,480	0,485	[illegible]	0,495

$^{o}/D_\infty = 0.0035$

3

Source length

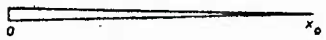

Half body of the linear source length with $R_o^2/X_o^2 = 0.04$

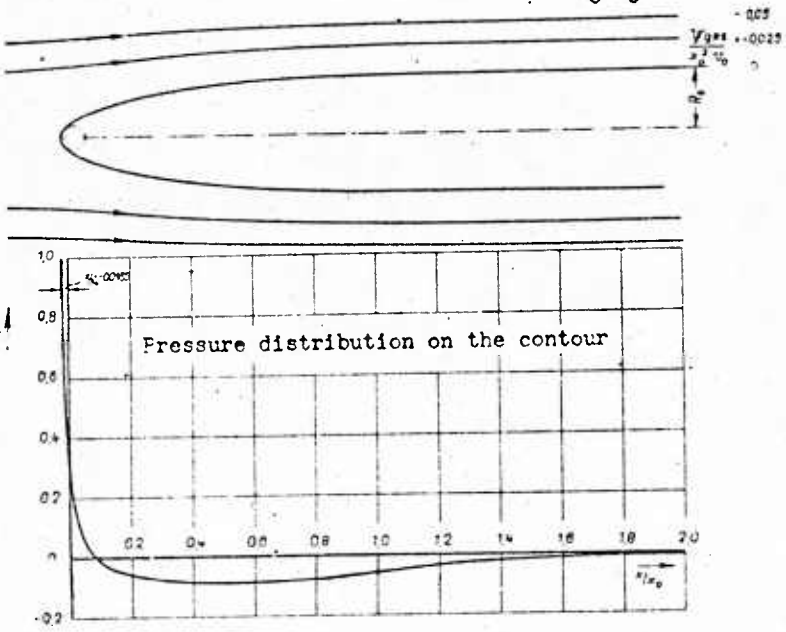

x/l_{∞}	0	005	010	015	020	030	040	050	075	100	125	150	175	200	250	300	350	400	500
y/l_{∞}	0	0293	01	0155	0180	0220	0255	0285	03	0387	0423	0	0	0	0	0	0	0	0

$\delta/l_{\infty} = 0103$

4

Source length

Half body of the second power source length with $R_o^2/X_o^2 = 0.04$

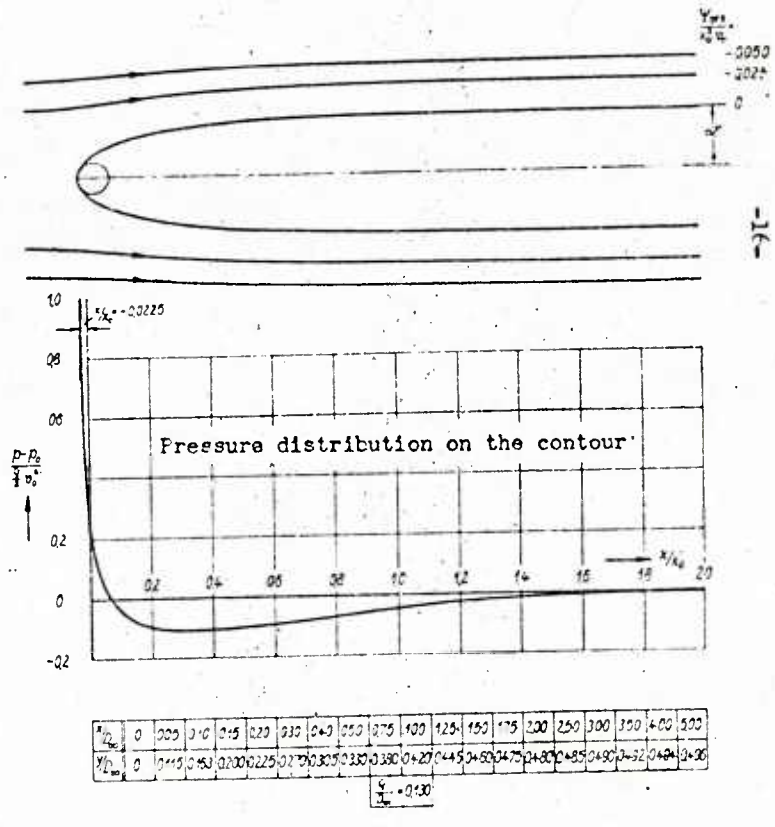

x/l_{∞}	0	005	010	015	020	030	040	050	075	100	125	150	175	200	250	300	350	400	500
y/l_{∞}	0	0145	0193	0200	0225	027	0305	0330	0380	0420	0	0	0	0	0	0	0	0	0

$\frac{\delta}{l_{\infty}} = 0130$

5

Source length

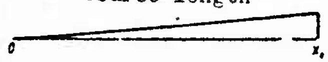

Half body of the linear source length with $R_o^2/X_o^2 = 0.09$

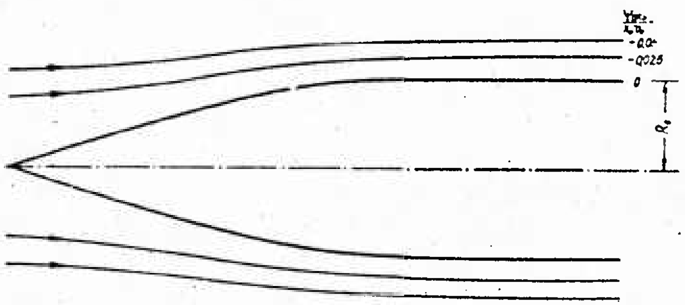

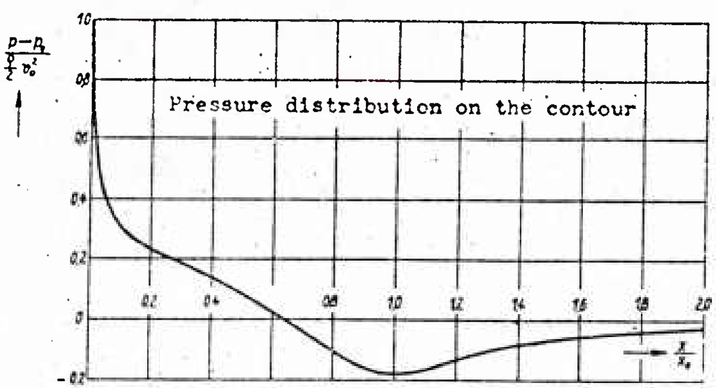

x/x_o	0	0.05	0.10	0.15	0.20	0.25	0.30	0.40	0.50	0.60	0.70	0.80	0.90	1.00	1.30	1.60	2.00	2.50	3.00
y/x_o	0	0.017	0.033	0.050	0.067	0.083	0.100	0.127	0.163	0.192	0.220	0.252	0.282	0.310	[illegible]	[illegible]	0.480	0.490	0.495

6

Source length

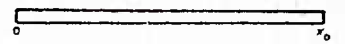

Half body of the constant source length with $R_o^2/X_o^2 = 0.09$

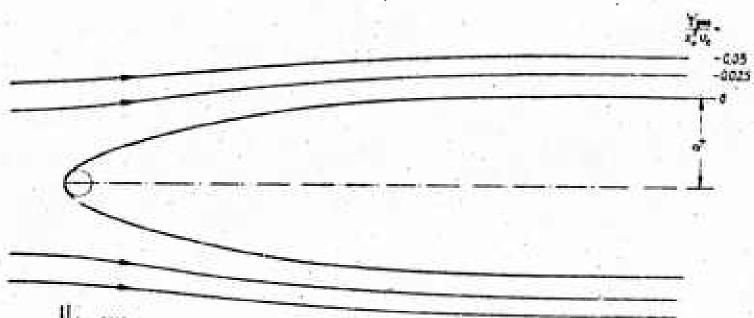

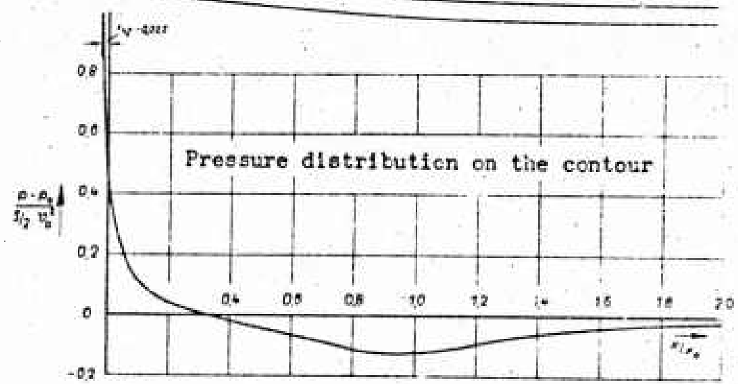

x/a	0	0.05	0.10	0.15	0.20	0.25	0.30	0.40	0.50	0.60	0.70	0.80	0.90	1.00	1.30	1.50	2.00	2.50	3.00
y/a	0	0.085	0.118	0.143	0.167	0.185	0.206	0.255	[illegible]	[illegible]	0.315	0.335	[illegible]	0.377	0.421	0.455	0.480	0.485	0.490

$s/a = 0.069$

7

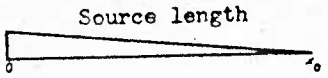

Half body of the linear source length with $R_o^2/X_o^2 = 0.09$

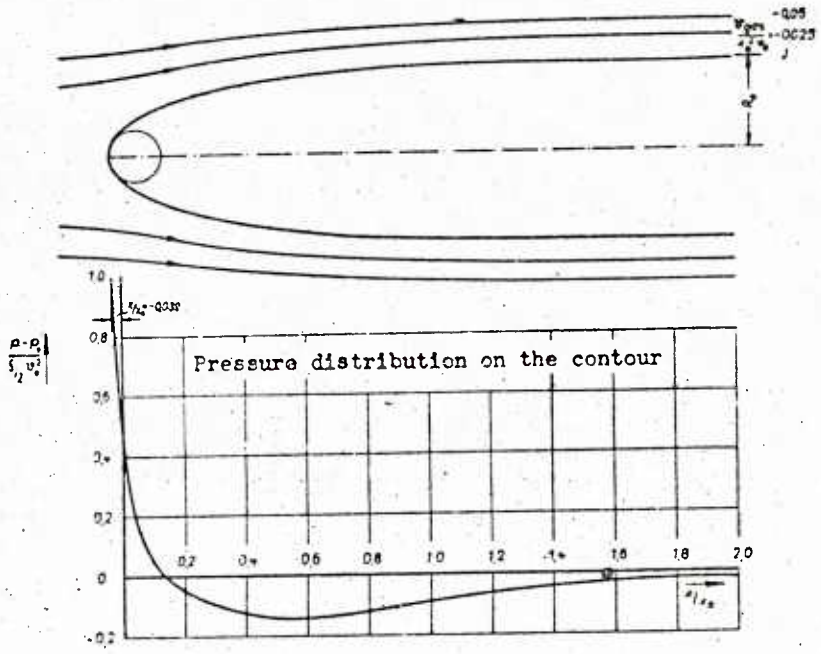

x/D_m	0	0.05	0.10	0.15	0.20	0.25	0.30	0.40	0.50	0.60	0.70	0.80	0.90	1.00	1.50	1.80	2.00	2.50	3.00
y/D_m	0	0.116	0.167	0.202	0.227	0.250	0.270	0.30+	0.33	0.36	0.38	0.40+	0.42+	0.44+	0.50+	0.53+	0.55+	0.58+	0.62+

$\rho_1/D_m = 0.140$

8

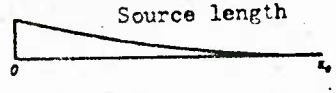

Half body of the second-power source length with $R_o^2/X_o^2 = 0.09$

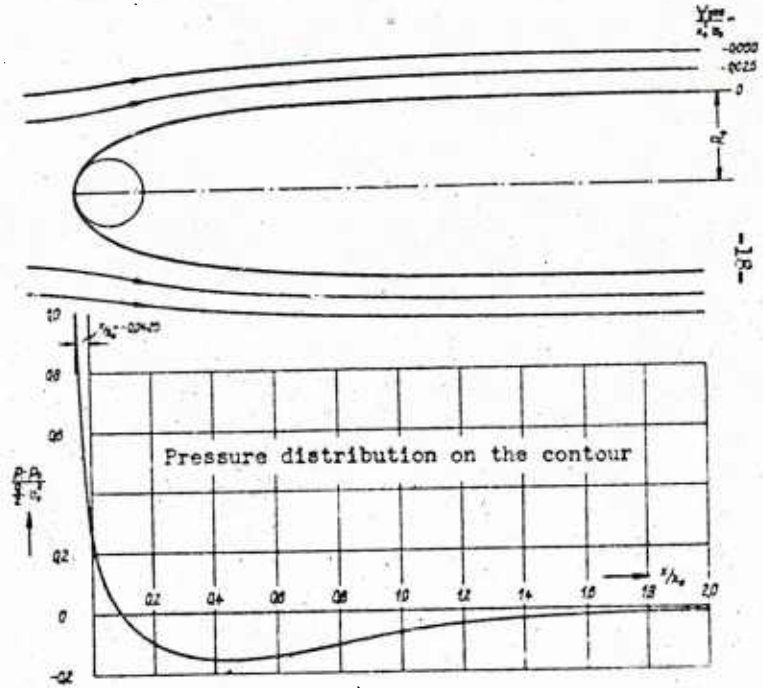

x/D_m	0	0.05	0.10	0.15	0.20	0.25	0.30	0.40	0.50	0.60	0.70	0.80	0.90	1.00	1.30	1.60	2.00	2.50	3.00
y/D_m	0	0.04+	0.09	0.12	0.15	0.18	0.20	0.23	0.25	0.27	0.29	0.30+	0.32+	0.33+	0.36+	0.38+	0.40+	0.42+	0.43+

$\rho_1/D_m = 0.152$

9

Source length

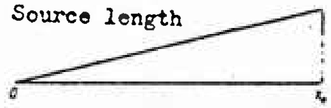

Half body of the linear source length with $R_o^2/X_o^2 = 0.25$

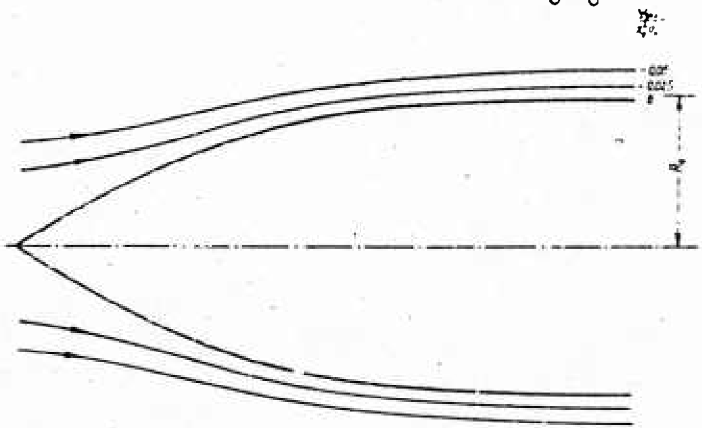

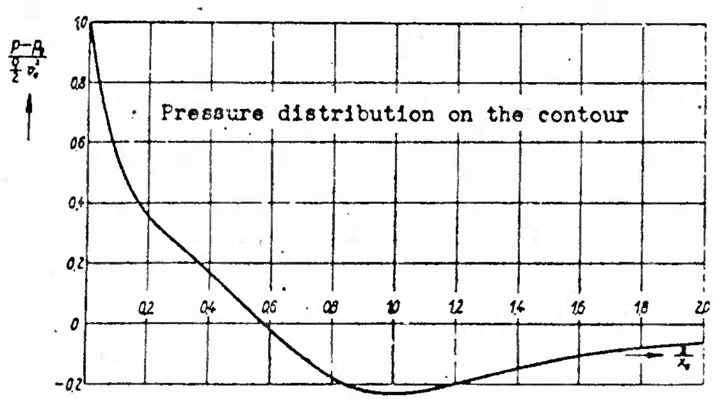

x/l	0	0,02	0,04	0,06	0,08	0,10	0,15	0,20	0,30	0,40	0,50	0,60	0,80	1,00	1,20	1,40	1,60	1,80	2,00
y/l	0	0,013	0,025	0,039	0,052	0,065	0,098	0,128	0,180	0,230	0,280	0,326	0,392	0,435	0,462	0,476	0,485	[illegible]	0,490

10

Source length

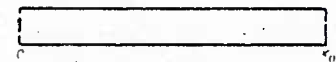

Half body of the constant source length with $R_o^2/X_o^2 = 0.25$

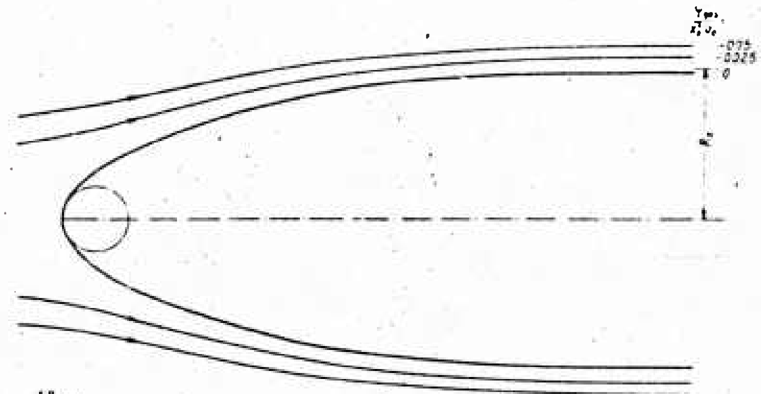

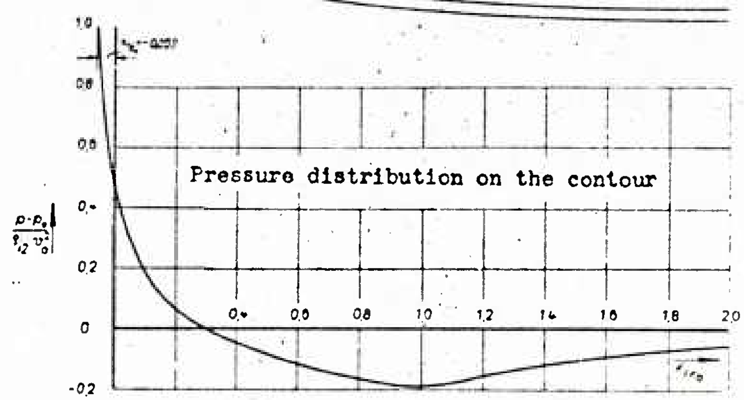

x/D	0	[illegible]	0,04	0,06	0,08	0,10	0,15	0,20	0,30	0,40	0,50	0,60	0,80	1,00	1,20	1,40	1,60	1,80	2,00
y/D	0	0,061	0,090	0,115	0,152	0,150	0,185	0,212	0,259	0,296	0,350	0,381	0,412	0,430	0,467	0,475	[illegible]	0,486	0,490

y/D = 0,110

11

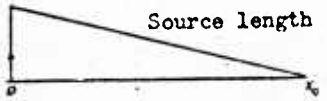

Half body of the linear source length with $R_o^2/X_o^2 = 0.25$

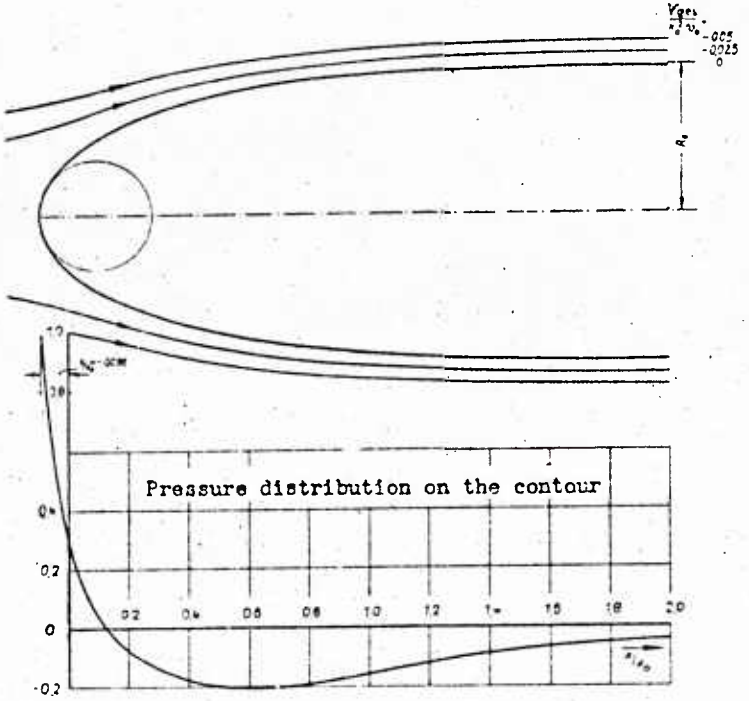

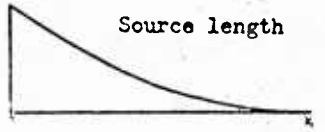

Half body of the second-power source length with $R_o^2/X_o^2 = 0.25$

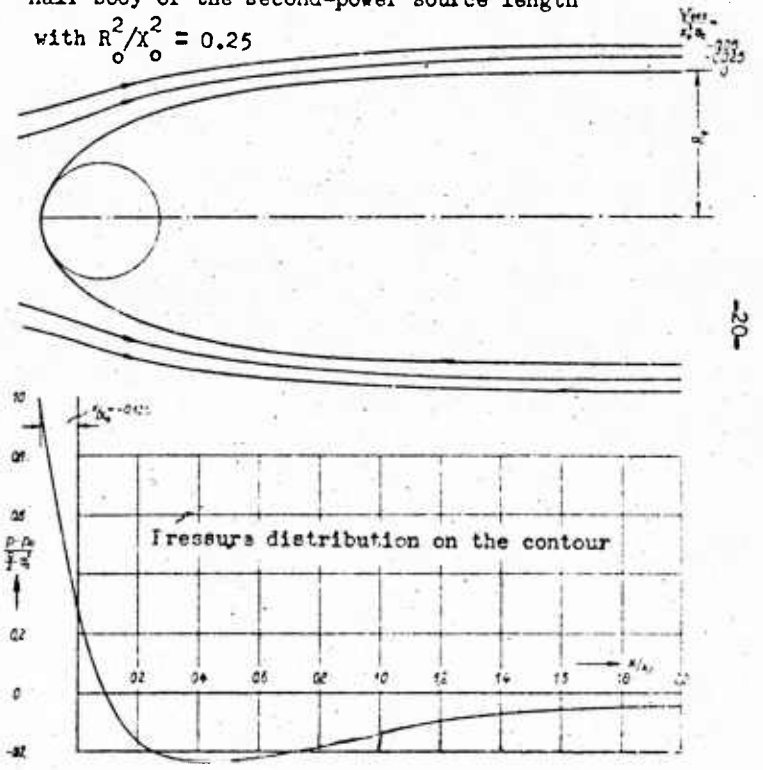

-20-

I_1

Source-sink distribution

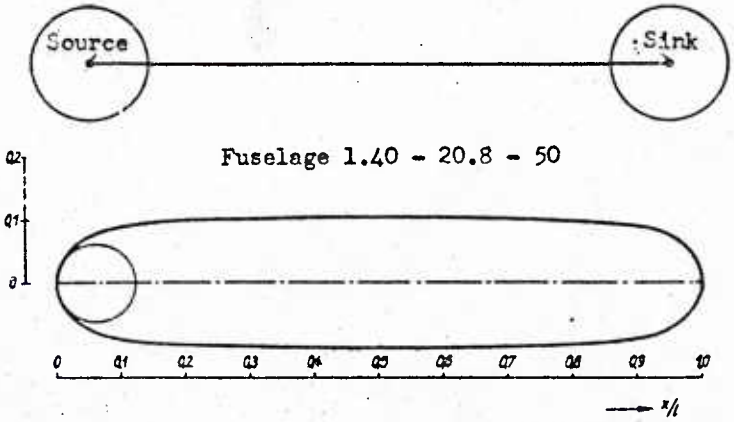

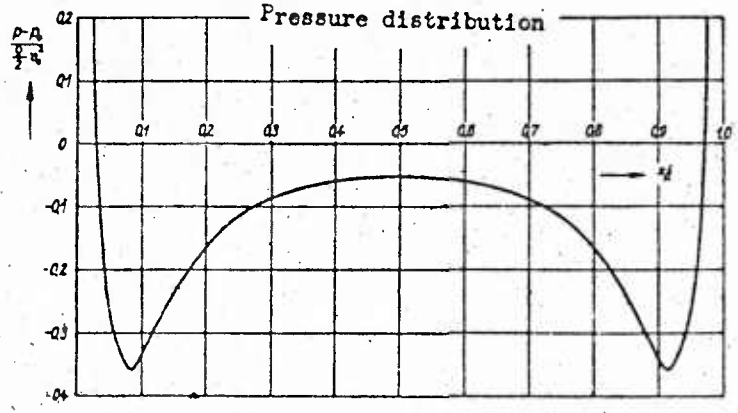

x/l	0	0.01	0.02	0.03	0.04	0.06	0.08	0.10	0.12	0.14	0.16	0.18	0.20	0.25	0.30	0.35	0.40	0.45	0.50
y/l	0																		

$\frac{\rho}{2} = 140 \frac{d^2}{l^2}$

I_2

Source-sink distribution

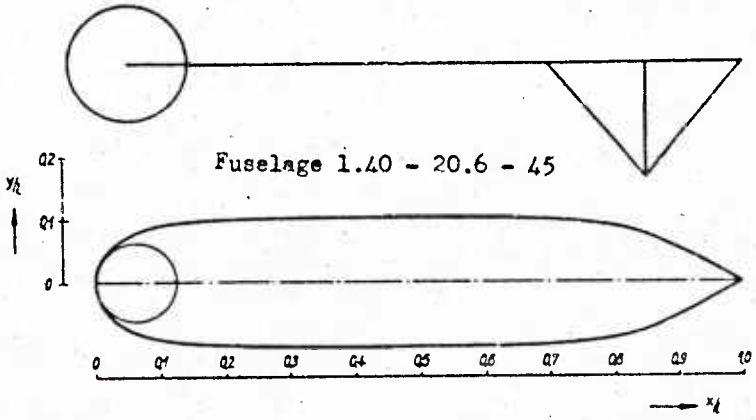

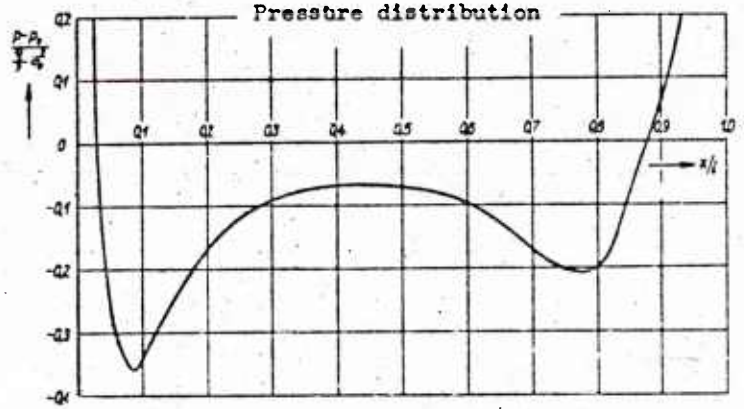

x/l	0	0.01	0.02	0.03	0.04	0.06	0.08	0.10	0.15	0.20	0.30	0.40	0.50	0.60	0.70	0.80	0.90	0.95	1.00
y/l	0																		0

$\frac{\rho}{2} = 140 \frac{d^2}{l^2}$

I_3

Source-sink distribution

Fuselage 1.40 - 20.4 - 40

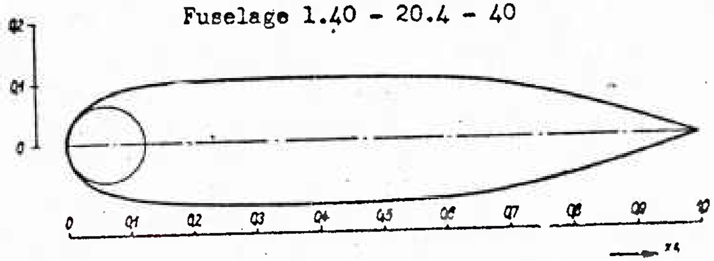

Pressure distribution

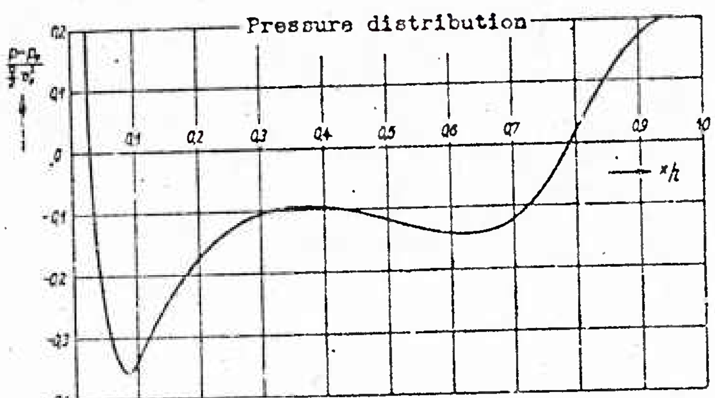

x/l	0	0.01	0.02	0.03	0.04	0.05	[illegible]	0.10	0.15	0.20	0.30	0.40	0.50	0.60	0.70	0.80	0.90	0.95	1.00
y/l	0	[illegible]	[illegible]	[illegible]	[illegible]	[illegible]	[illegible]	[illegible]	[illegible]	[illegible]	[illegible]	[illegible]	[illegible]	[illegible]	[illegible]	[illegible]	[illegible]	[illegible]	0

q/l · 1.40 [illegible]

I_4

Source-sink distribution

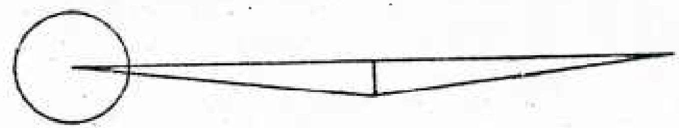

Fuselage 1.40 - 20 - 22

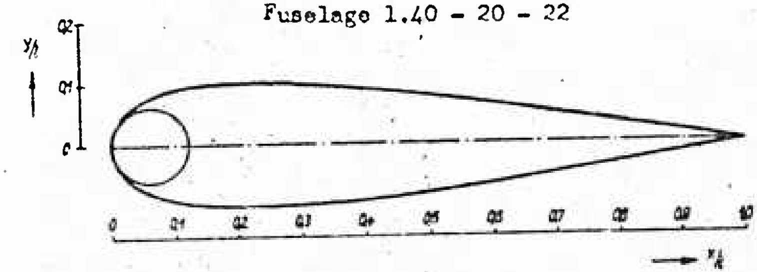

Pressure distribution

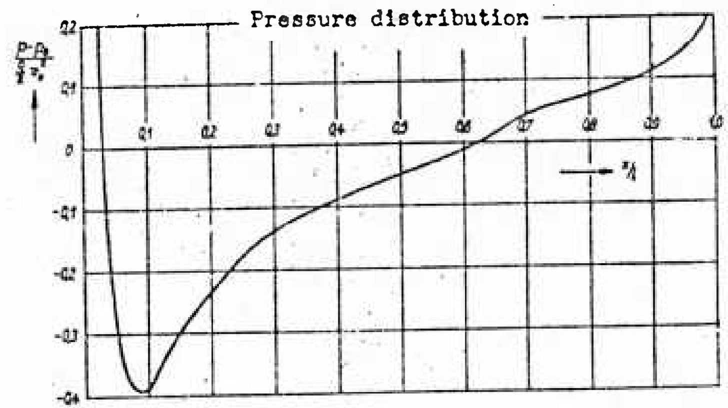

x/l	0	0.01	0.02	0.03	0.04	0.06	0.08	0.10	0.15	0.20	0.30	0.40	0.50	0.60	0.70	0.80	0.90	0.95	1.00
y/l	0	[illegible]	[illegible]	[illegible]	[illegible]	0.078	0.085	0.089	[illegible]	[illegible]	[illegible]	[illegible]	[illegible]	[illegible]	[illegible]	[illegible]	[illegible]	[illegible]	0

q/l · 1.40 [illegible]

II.1

Source-sink distribution

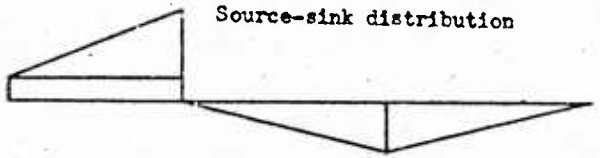

Fuselage 0.12 - 20.4 - 40

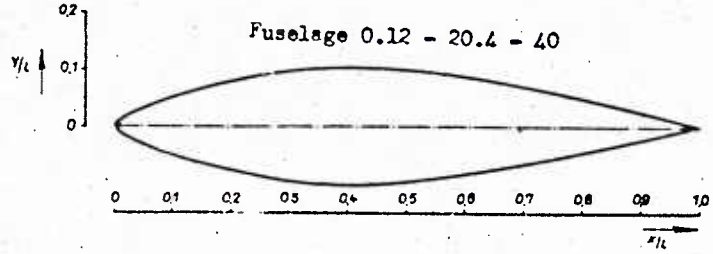

Pressure distribution

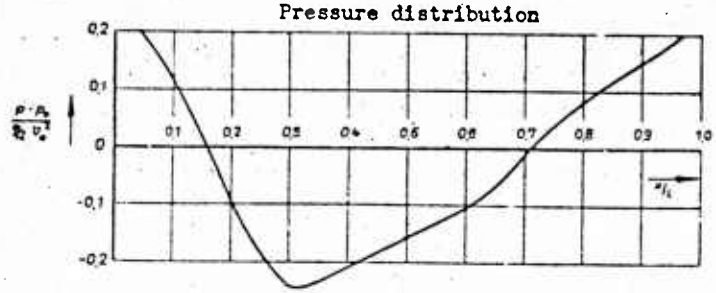

x/l	0	0,01	0,02	0,03	0,04	0,06	0,08	0,10	0,15	0,20	0,30	0,40	0,50	0,60	0,70	0,80	0,90	0,95	1,00
y/l	0	0,010	0,014	0,018	0,022	0,027	0,031	0,035	0,043	0,050	0,060	0,067	0,072	0,075	0,076	0,074	0,068	0,060	0

$\pm 0{,}12 \frac{d}{l}$

II.2

Source-sink distribution

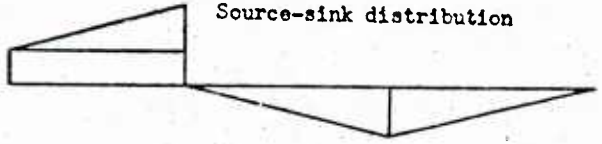

Fuselage 0.34 - 20.4 - 40

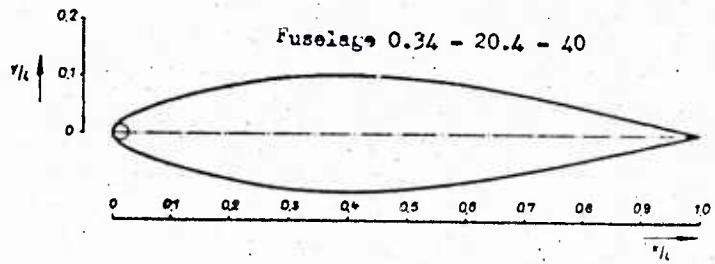

Pressure distribution

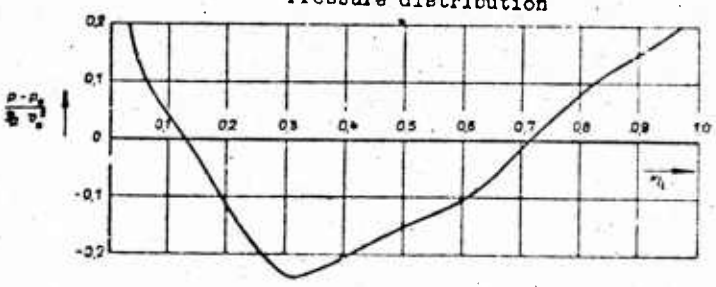

x/l	0	0,01	0,02	0,03	0,04	0,06	0,08	0,10	0,15	0,20	0,30	0,40	0,50	0,60	0,70	0,80	0,90	0,95	1,00
y/l	0	0,016	0,023	0,028	0,033	0,040	0,045	0,050	0,060	0,068	0,078	0,085	0,090	0,092	0,092	0,090	0,084	0,077	0

$\pm 0{,}34 \frac{d}{l}$

II3

Source-sink distribution

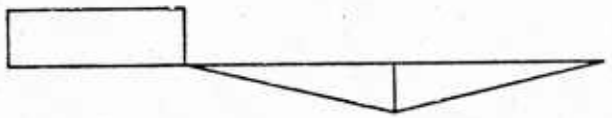

Fuselage 0.46 - 20 - 40

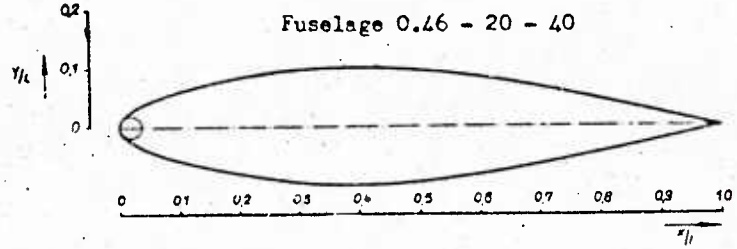

Pressure distribution

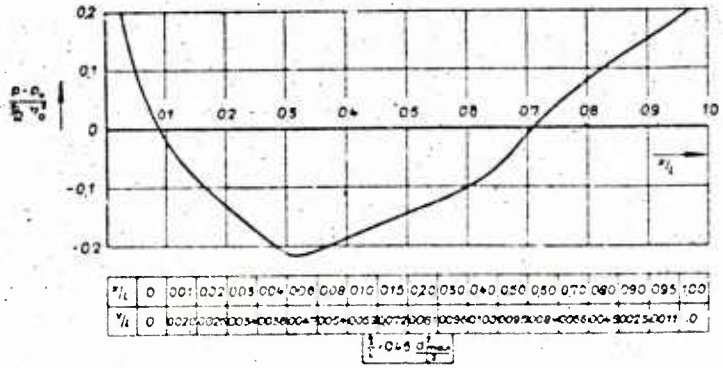

x/l	0	001	002	003	004	006	008	010	015	020	030	040	050	060	070	080	090	095	100
y/l	0	002	003	004	005	006	007	008	010	012	015	018	020	022	024	025	026	027	0

$\frac{I}{l} \cdot 046 \frac{d}{l^2} \frac{f_{max}}{l}$

II4

Source-sink distribution

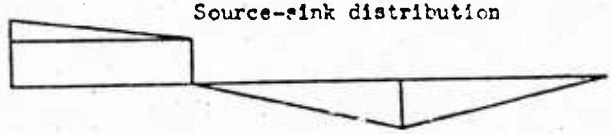

Fuselage 0.55 - 20 - 40

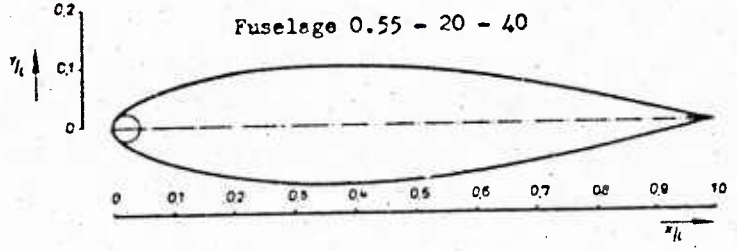

Pressure distribution

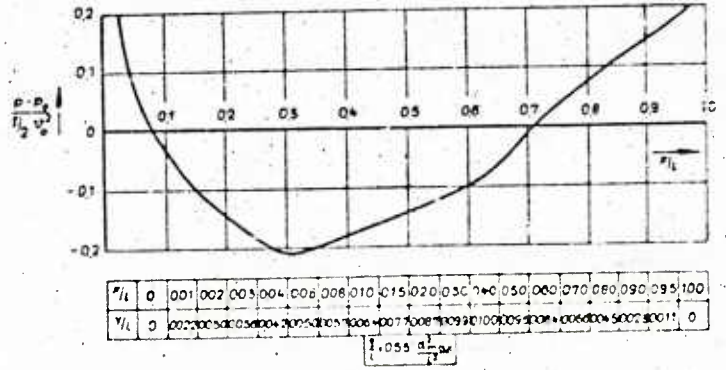

x/l	0	001	002	003	004	006	008	010	015	020	030	040	050	060	070	080	090	095	100
y/l	0	002	003	004	005	006	007	008	010	012	015	018	020	022	024	025	026	027	0

$\frac{I}{l} \cdot 055 \frac{d}{l^2} \frac{f_{max}}{l}$

II5

Source-sink distribution

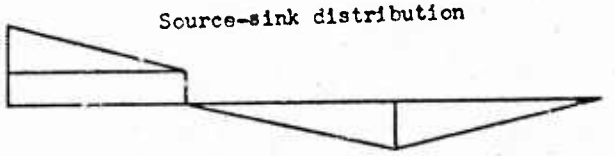

Fuselage 0.61 - 20.2 - 40

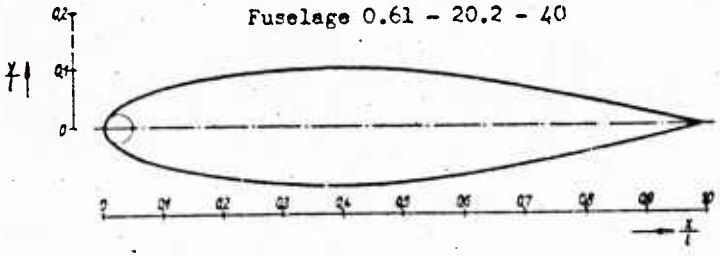

Pressure distribution

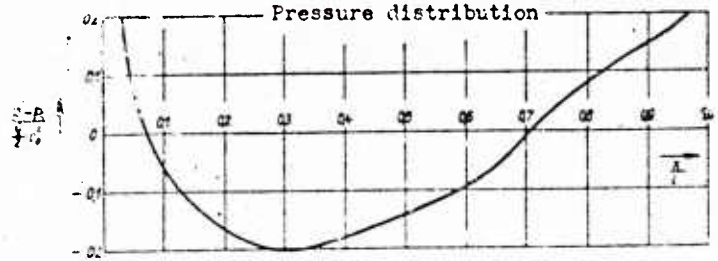

$\frac{x}{l}$	0	0.01	0.02	0.03	0.04	0.06	0.08	0.10	0.15	0.20	0.30	0.40	0.50	0.60	0.70	0.80	0.90	0.95	1.00
$\frac{y}{l}$	0	0.0037	0.0052	0.0064	0.0073	0.0087	0.0097	0.0105	0.0125	0.0138	0.0158	0.0171	0.0177	0.0174	0.0166	0.0145	0.0113	0.0091	0

$\frac{c}{l} = 0.61 \quad \frac{\Omega'_{max}}{l^2}$

II6

Source-sink distribution

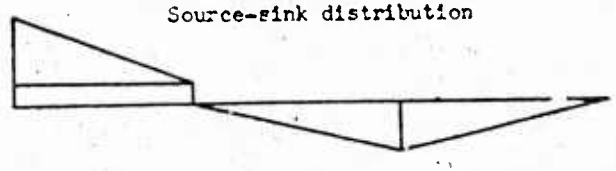

Fuselage 0.61 - 20.4 - 38

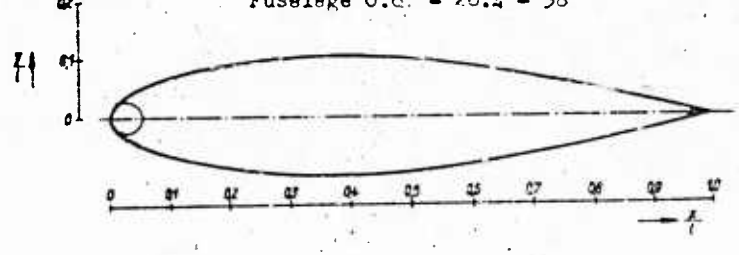

Pressure distribution

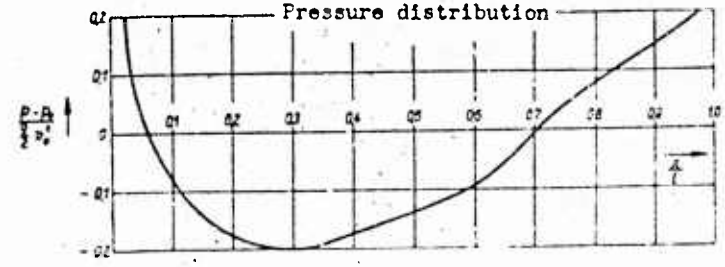

$\frac{x}{l}$	0	0.01	0.02	0.03	0.04	0.06	0.08	0.10	0.15	0.20	0.30	0.40	0.50	0.60	0.70	0.80	0.90	0.95	1.00
$\frac{y}{l}$	0	0.0034	0.0047	0.0057	0.0064	0.0076	0.0084	0.0090	0.0103	0.0112	0.0126	0.0134	0.0137	0.0134	0.0126	0.0109	0.0085	0.0068	0

$\frac{c}{l} = 0.67 \quad \frac{\Omega'_{max}}{l^2}$

II 7

Source-sink distribution

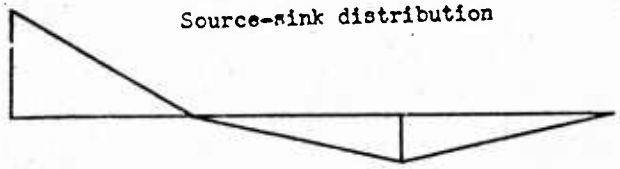

Fuselage 0.80 - 20 - 35

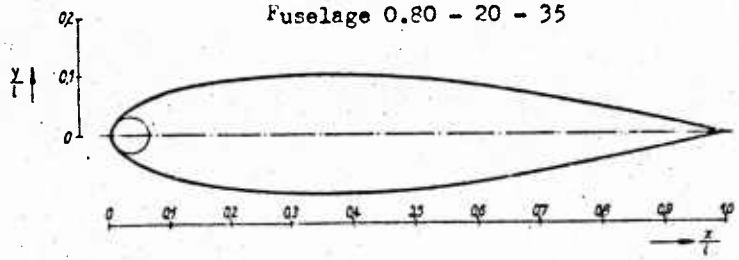

Pressure distribution

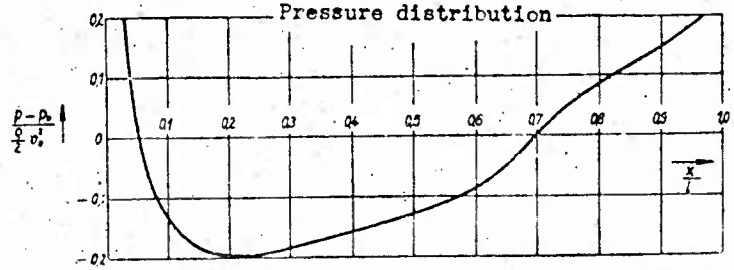

x/l	0	0.01	0.02	0.03	0.04	0.06	0.08	0.10	0.15	0.20	0.30	0.40	0.50	0.60	0.70	0.80	0.90	0.95	1.00
y/l	0	0.0225	0.0315	0.0374	0.0418	0.0485	0.0535	0.0573	0.0637	0.0682	0.0736	0.0758	0.0753	0.0727	0.0664	0.0574	0.0427	0.0311	0

$\frac{Q}{l} = 0.80 \quad \frac{d^2 m a s}{l}$

II 8

Source-sink distribution

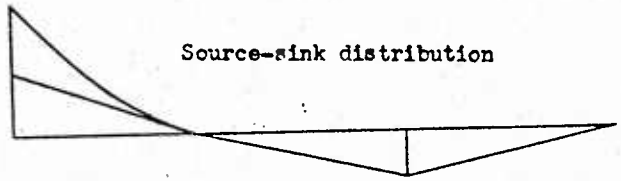

Fuselage 0.85 - 20 - 35

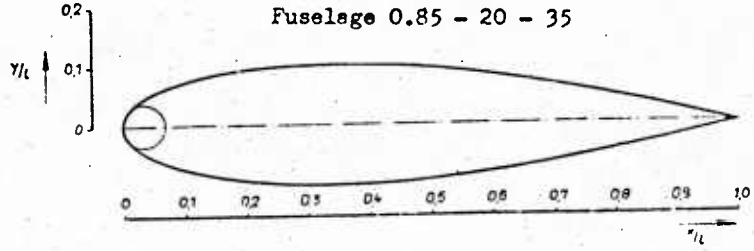

Pressure distribution

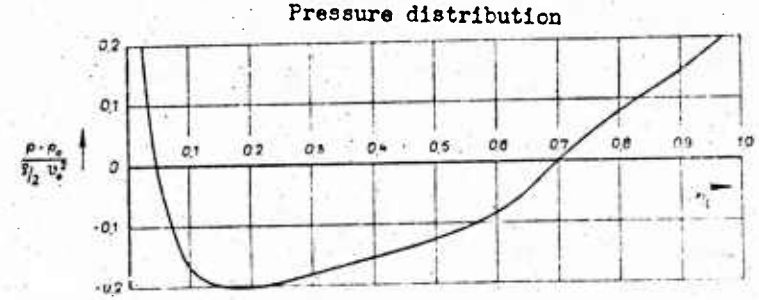

x/l	0	0.01	0.02	0.03	0.04	0.06	0.08	0.10	0.15	0.20	0.30	0.40	0.50	0.60	0.70	0.80	0.90	0.95	1.00
y/l	0	0.0271	0.0357	0.0414	0.0457	0.0523	0.0573	0.0611	0.0675	0.0720	0.0774	0.0796	0.0791	0.0765	0.0702	0.0612	0.0465	0.0349	0

$\frac{Q}{l} = 0.85 \quad \frac{d^2 m a s}{l}$

III 1 Source-sink distribution

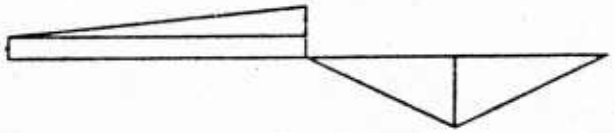

Fuselage 0.14 - 20 - 50

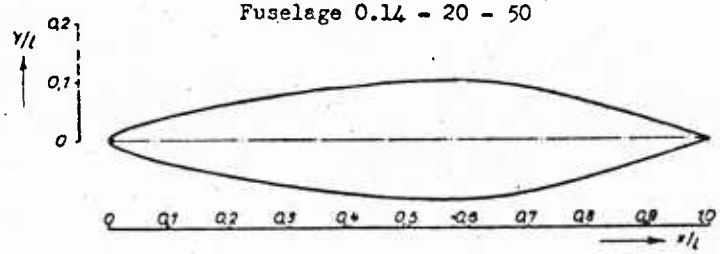

Pressure distribution

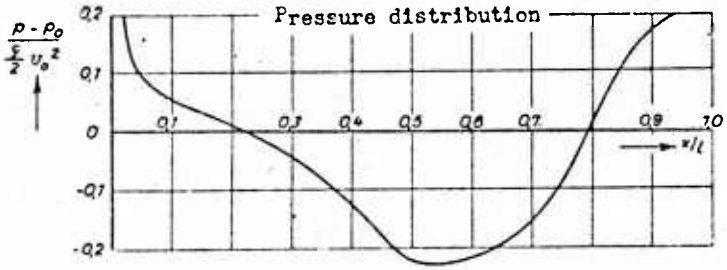

x/l	0	0,01	0,02	0,03	0,04	0,06	0,08	0,10	0,15	0,20	0,30	0,40	0,50	0,60	0,70	0,80	0,90	0,95	1,00
Y/l	0	0,030	0,042	0,051	0,058	0,069	0,078	0,085	0,098	0,107	0,120	0,126	0,128	0,126	0,120	0,107	0,085	0,058	0

$\frac{f}{l} = 0{,}14 \quad \frac{z^2}{l^2}$

III 2 Source-sink distribution

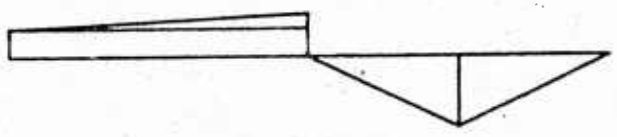

Fuselage 0.22 - 20 - 50

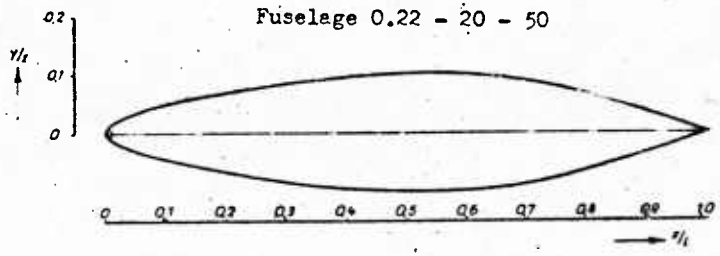

Pressure distribution

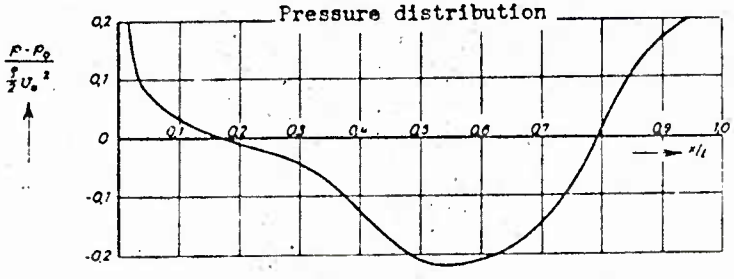

x/l	0	0,01	0,02	0,03	0,04	0,06	0,08	0,10	0,15	0,20	0,30	0,40	0,50	0,60	0,70	0,80	0,90	0,95	1,00
Y/l	0	0,047	0,065	0,080	0,091	0,108	0,122	0,133	0,154	0,168	0,189	0,198	0,201	0,198	0,189	0,168	0,133	0,091	0

$\frac{f}{l} = 0{,}22 \quad \frac{z^2}{l^2}$

III 3 Source-sink distribution

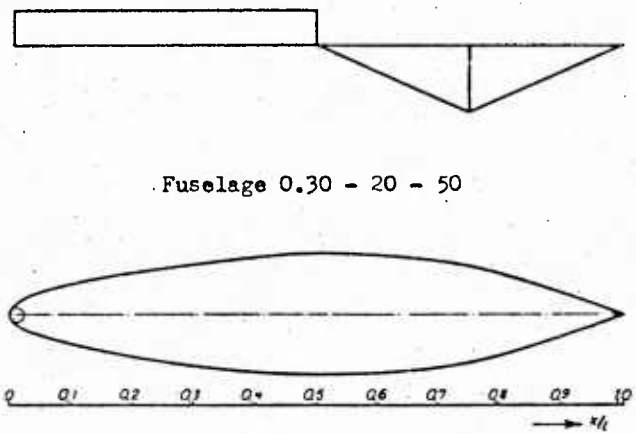

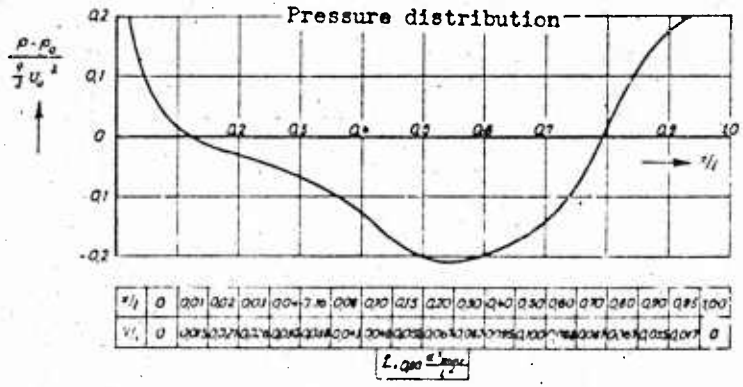

x/l	0	0.01	0.02	0.03	0.04	0.06	0.08	0.10	0.15	0.20	0.30	0.40	0.50	0.60	0.70	0.80	0.90	0.95	1.00
y/l	0																		0

f . 0,30 a²/l

III 4 Source-sink distribution

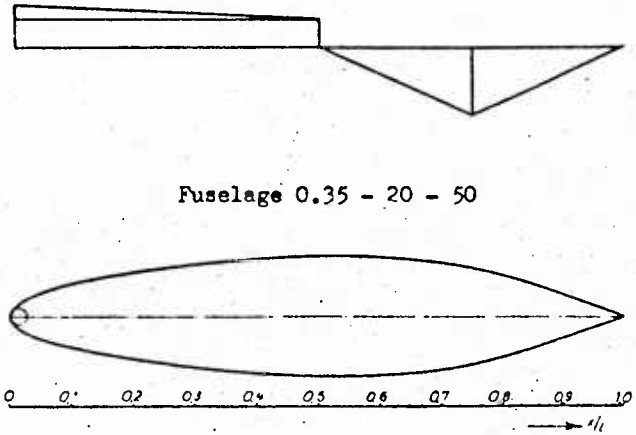

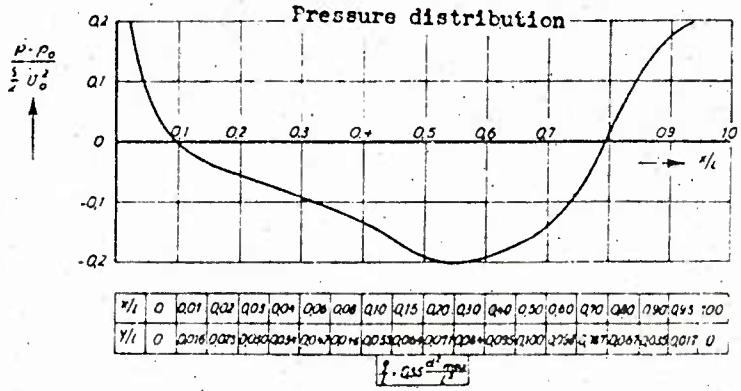

x/l	0	0.01	0.02	0.03	0.04	0.06	0.08	0.10	0.15	0.20	0.30	0.40	0.50	0.60	0.70	0.80	0.90	0.95	1.00
y/l	0																		0

f . 0,35 a²/l

III5

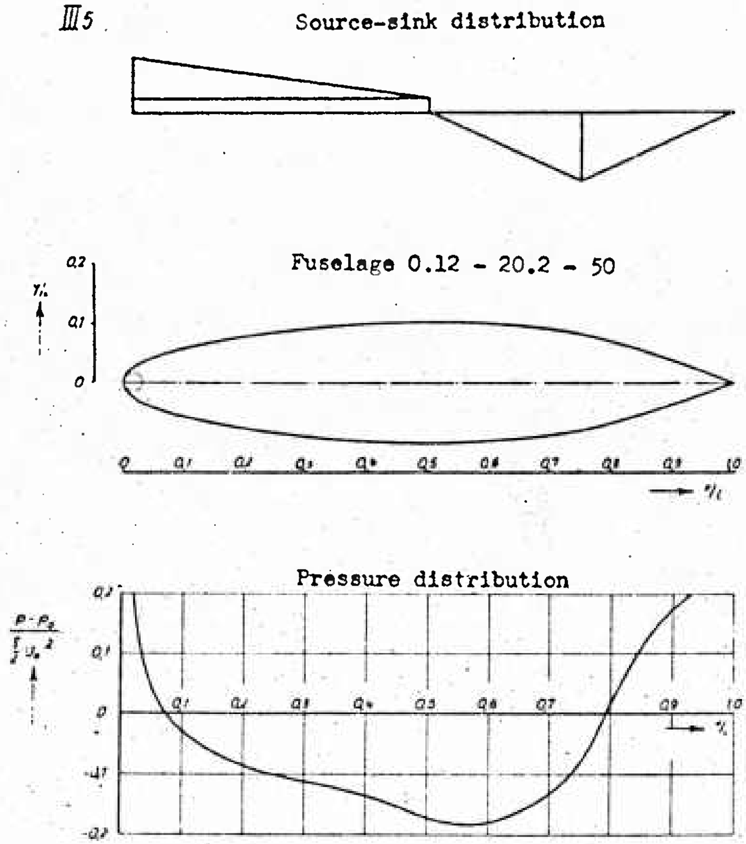

x/l	0	0,01	0,02	0,03	0,04	0,06	0,08	0,10	0,15	0,20	0,30	0,40	0,50	0,60	0,70	0,80	0,90	0,95	1,00
Y/l	0	0,017	0,026	0,033	0,037	0,04[illegible]	0,054	0,055	0,064	0,075	0,085	0,094	0,101	0,096	0,087	0,065	0,035	0,017	0

$\frac{\rho}{l} = 0.12 \frac{d^2_{max}}{l^2}$

III6

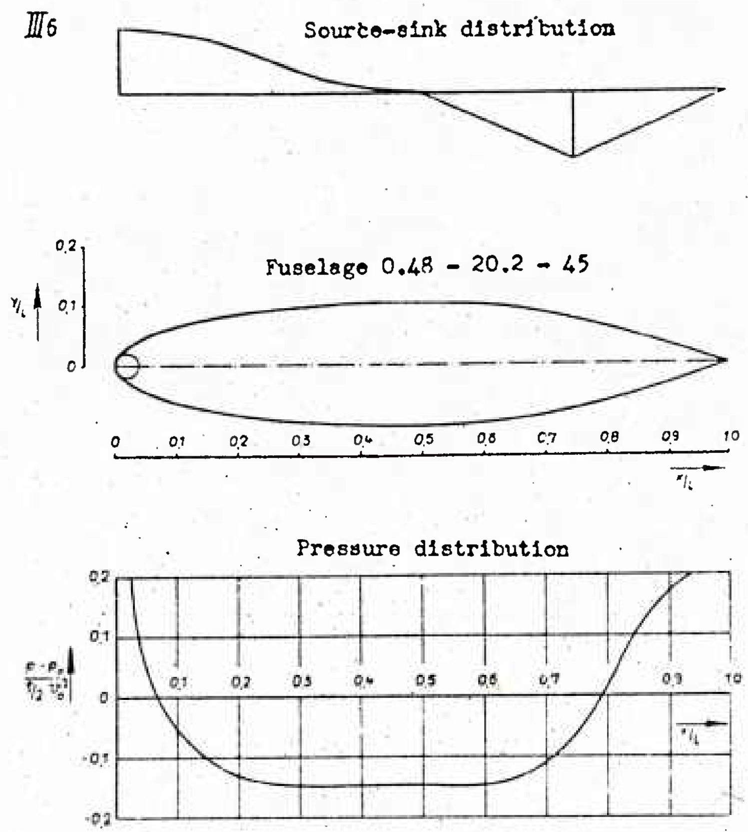

x/l	0	0,01	0,02	0,03	0,04	0,06	0,08	0,10	0,15	0,20	0,30	0,40	0,50	0,60	0,70	0,80	0,90	0,95	1,00
Y/l	0	0,020	0,026	0,034	0,040	0,050	0,058	0,065	0,075	0,085	0,095	0,100	0,100	0,097	0,085	0,062	0,032	0,016	0

$\frac{\rho}{l} = 0.48 \frac{d^2_{max}}{l^2}$

III 7

Source-sink distribution

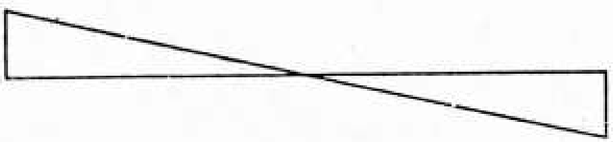

Fuselage 0.50 - 20.4 - 50

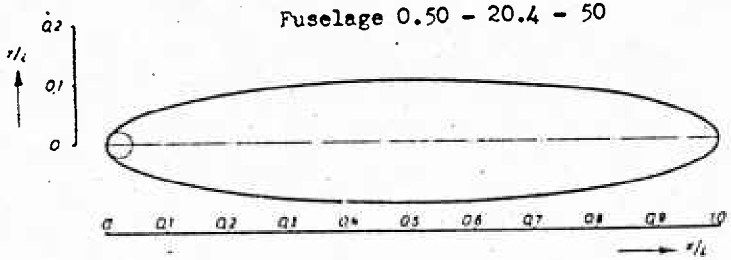

Pressure distribution

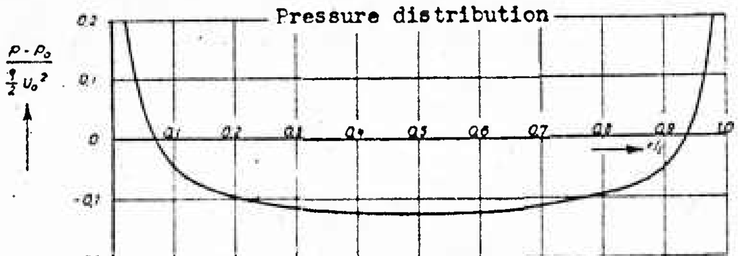

x/l	0	0.01	0.02	0.03	0.04	0.06	0.08	0.10	0.15	0.20	0.30	0.40	0.50	0.60	0.70	0.80	0.90	0.95	1.00
y/l	0	0.020	0.029	0.035	0.040	0.044	0.055	0.061	0.075	0.087	0.094	[illegible]	0.102	0.100	0.094	0.082	0.061	0.044	0

$\frac{V}{l^3} = 0.50 \frac{d^2_{max}}{l^2}$

III 8

Source-sink distribution

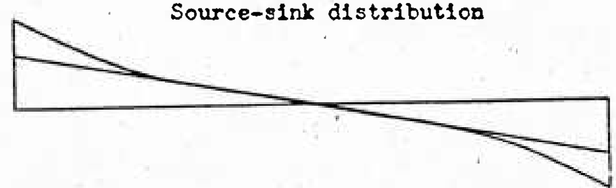

Fuselage 0.67 - 20 - 50

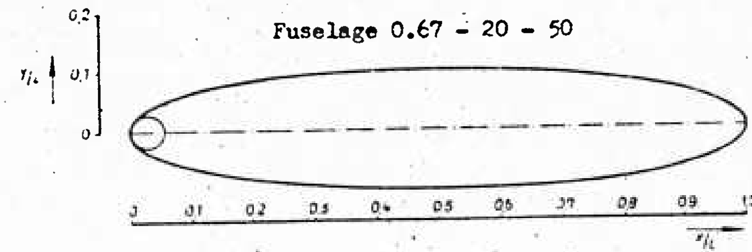

Pressure distribution

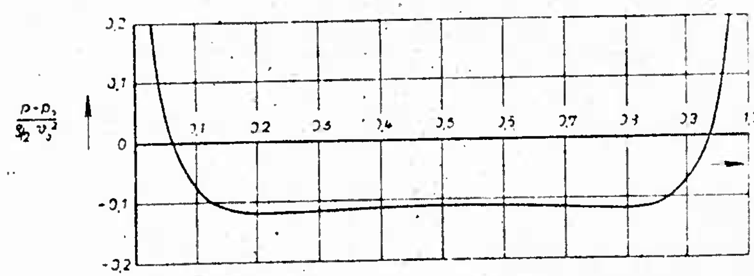

x/l	0	0.01	0.02	0.03	0.04	0.06	0.08	0.10	0.12	0.14	0.16	0.18	0.20	0.25	0.30	0.35	0.40	0.45	0.50
y/l	0	0.025	0.035	0.053	[illegible]	0.057	0.057	0.065	0.068	0.075	0.077	[illegible]	[illegible]	0.087	[illegible]	[illegible]	[illegible]	[illegible]	[illegible]

$\frac{V}{l^3} = 0.57\, d^2_{max}$

IV 1

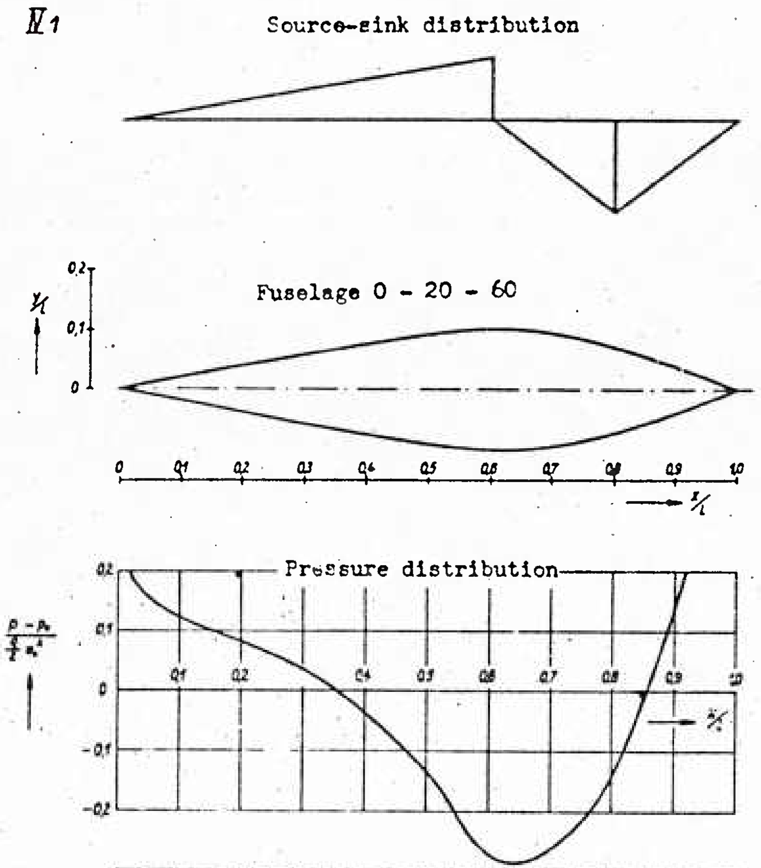

x/l	0	0,01	0,02	0,03	0,04	0,06	0,08	0,10	0,15	0,20	0,30	0,40	0,50	0,60	0,70	0,80	0,90	0,95	1,00
y/l	0	0,002	0,004	0,006	0,008	0,011	0,015	0,016	0,026	0,035	0,057	0,075	0,092	0,100	0,095	0,073	0,040	0,020	0

IV 2

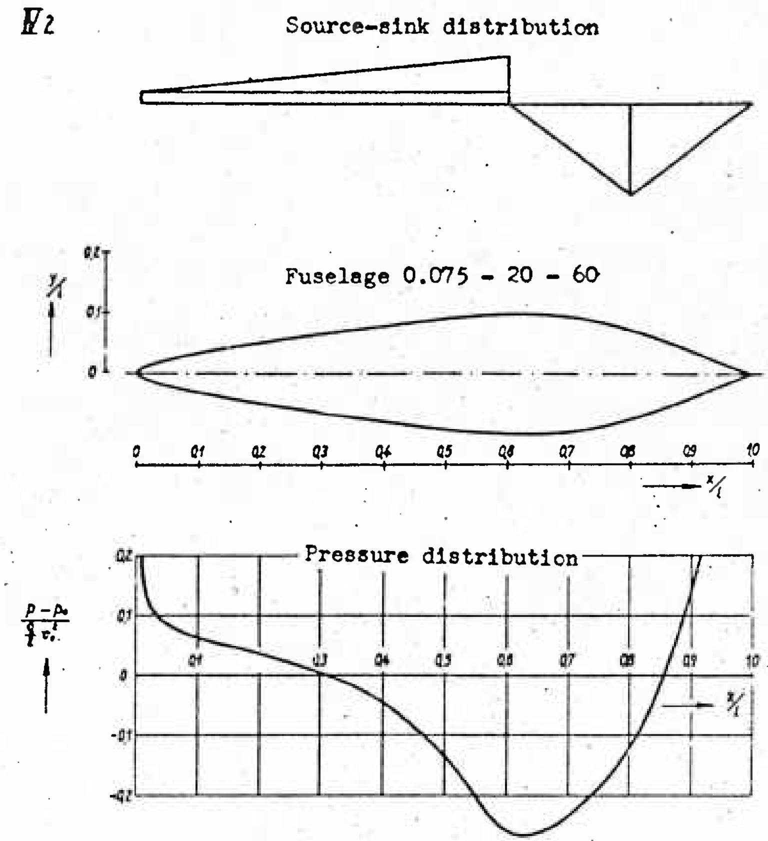

x/l	0	0,01	0,02	0,03	0,04	0,06	0,08	0,10	0,15	0,20	0,30	0,40	0,50	0,60	0,70	0,80	0,90	0,95	1,00
y/l	0	0,007	0,011	0,015	0,018	0,023	0,027	0,032	0,042	0,050	0,065	0,078	0,093	0,100	0,096	0,076	0,040	0,020	0

$\frac{\varrho}{l} = 0{,}075 \frac{d^2_{max}}{l^2}$

N3

Source-sink distribution

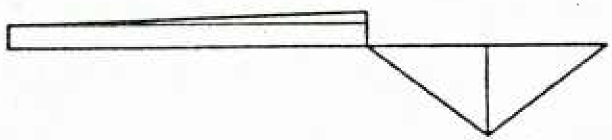

Fuselage 0.17 - 20.2 - 60

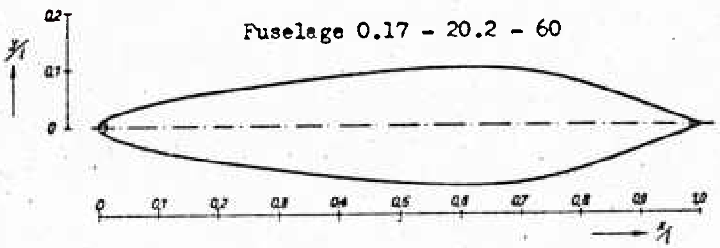

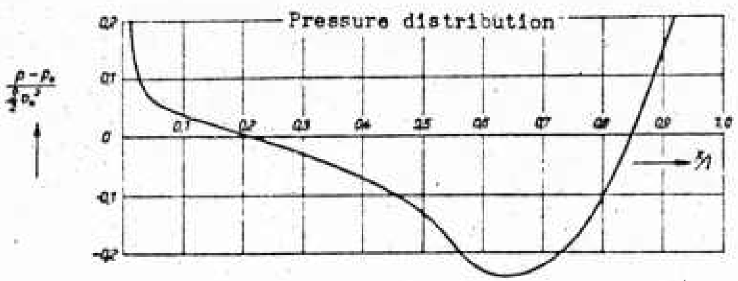

x/l	0	0,01	0,02	0,03	0,04	0,06	0,08	0,10	0,15	0,20	0,30	0,40	0,50	0,60	0,70	0,80	0,90	0,95	1,00
y/l	0	0,011	0,017	0,021	0,026	0,031	0,036	0,042	0,052	0,060	0,073	0,086	0,096	0,101	0,096	0,076	0,048	0,026	0

$\frac{\rho}{l} = 0{,}17\,\frac{d_{max}^2}{l^2}$

N4

Source-sink distribution

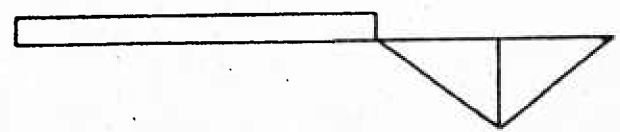

Fuselage 0.22 - 20.2 - 60

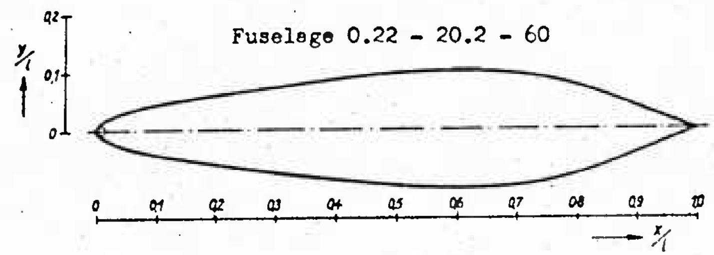

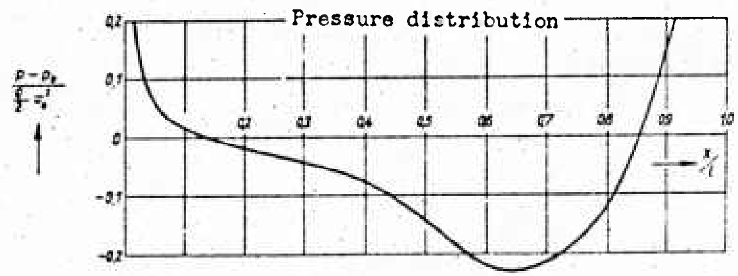

x/l	0	0,01	0,02	0,03	0,04	0,06	0,08	0,10	0,15	0,20	0,30	0,40	0,50	0,60	0,70	0,80	0,90	0,95	1,00
y/l	0	0,013	0,019	0,024	0,029	0,034	0,039	0,043	0,052	0,060	0,074	0,087	0,096	0,101	0,096	0,075	0,040	0,020	0

$\frac{\rho}{l} = 0{,}22\,\frac{d_{max}^2}{l^2}$

№ 5

Source-sink distribution

Fuselage 0.30 - 20 - 60

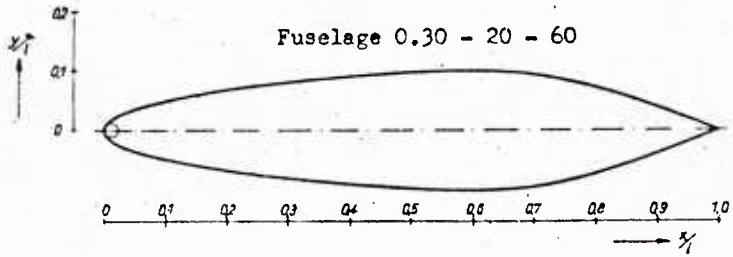

Pressure distribution

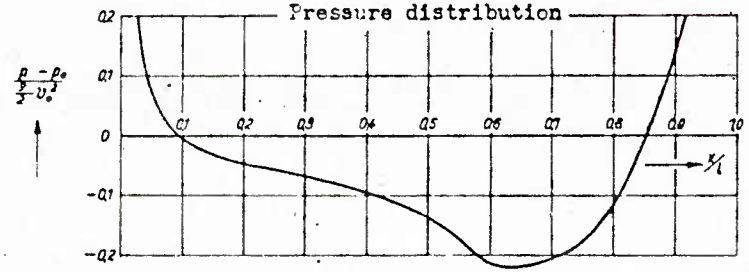

x/l	0	0.01	0.02	0.03	0.04	0.06	0.08	0.10	0.15	0.20	0.30	0.40	0.50	0.60	0.70	0.80	0.90	0.95	1.00
y/l	0	0.0175	0.027	0.0325	0.030	0.0337	0.0343	0.0345	0.0353	0.0357	0.0360	0.0350	0.0347	0.0330	0.0312	0.0272	0.0239	0.0220	0

$$\frac{\rho}{l} = 0.30 \frac{d^2 \frac{\rho}{\rho_\infty}}{l^2}$$

№ 6

Source-sink distribution

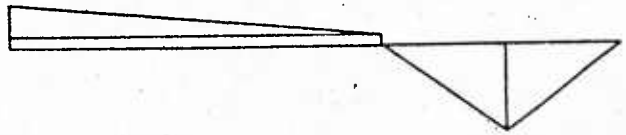

Fuselage 0.35 - 20 - 60

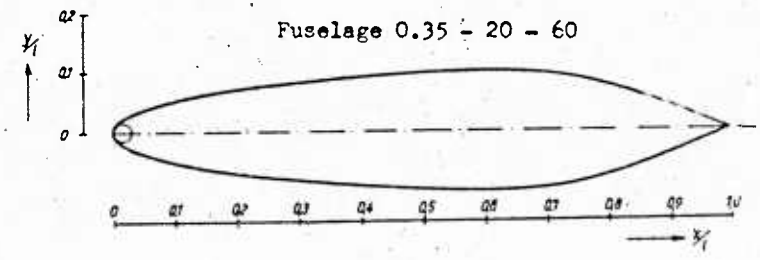

Pressure distribution

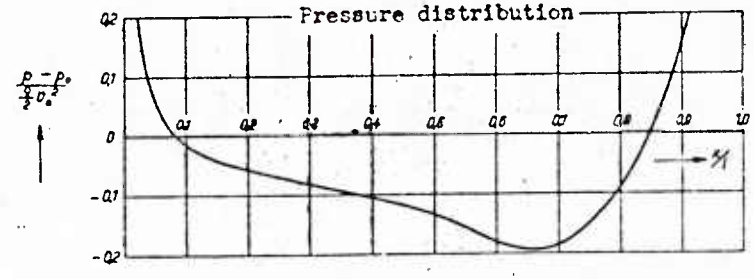

x/l	0	0.01	0.02	0.03	0.04	0.06	0.08	0.10	0.15	0.20	0.30	0.40	0.50	0.60	0.70	0.80	0.90	0.95	1.00
y/l	0	0.026	0.023	0.019	0.033	0.040	0.045	0.051	0.061	0.069	0.068	0.057	0.097	0.100	0.095	0.075	0.048	0.020	0

$$\frac{\rho}{l} = 0.35 \frac{d^2 \frac{\rho}{\rho_\infty}}{l^2}$$

№7

Source-sink distribution

Fuselage 0.40 - 20 - 55

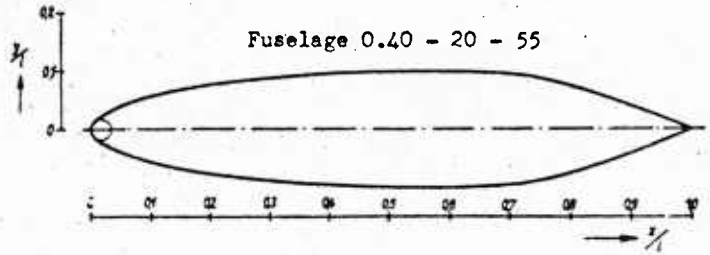

Pressure distribution

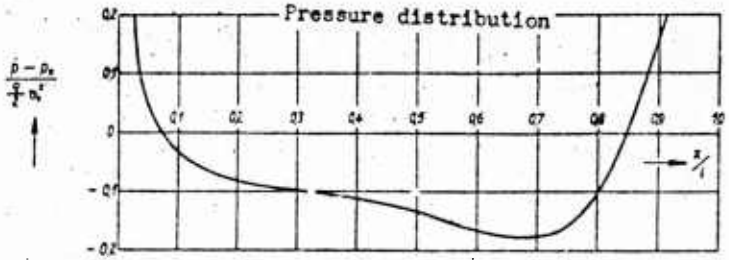

x/l	0	0.01	0.02	0.03	0.04	0.06	0.08	0.10	0.15	0.20	0.30	0.40	0.50	0.60	0.70	0.80	0.90	0.95	1.00
y/l	0	0.017	0.024	0.030	0.035	0.043	0.050	0.056	0.067	0.075	0.080	0.086	0.090	0.092	0.095	0.090	0.075	0.047	0.022	0

$\frac{q}{l} = 0.40 \frac{d_{max}}{l^2}$

№8

Source-sink distribution

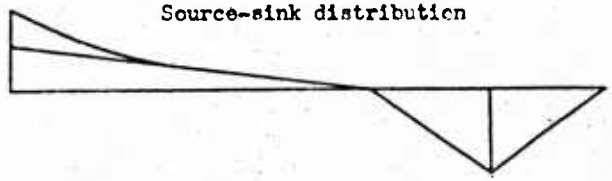

Fuselage 0.67 - 20 - 50

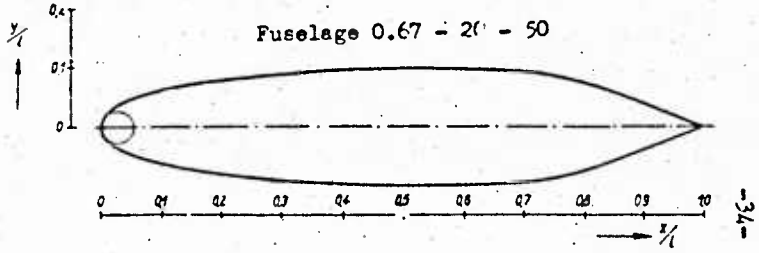

Pressure distribution

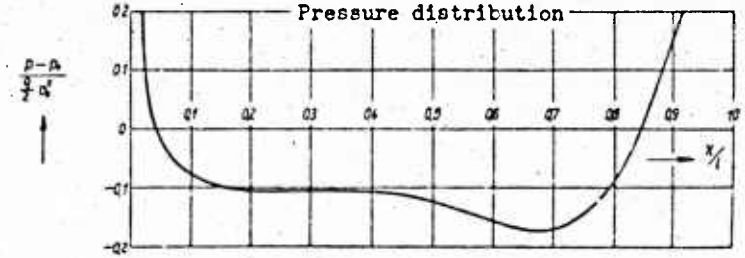

x/l	0	0.01	0.02	0.03	0.04	0.05	0.06	0.10	0.15	0.20	0.30	0.40	0.50	0.60	0.70	0.80	0.90	0.95	1.00
y/l	0	0.023	0.033	0.039	0.043	0.050	0.056	0.062	0.072	0.079	0.091	0.097	0.100	0.099	0.095	0.079	0.054	0.033	0

$\frac{q}{l} = 0.67 \frac{d_{max}}{l^2}$

№ 9

Source-sink distribution

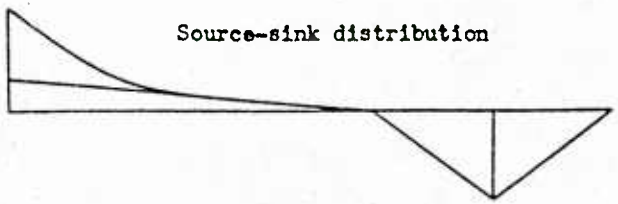

Fuselage 0.75 - 20.4 - 50

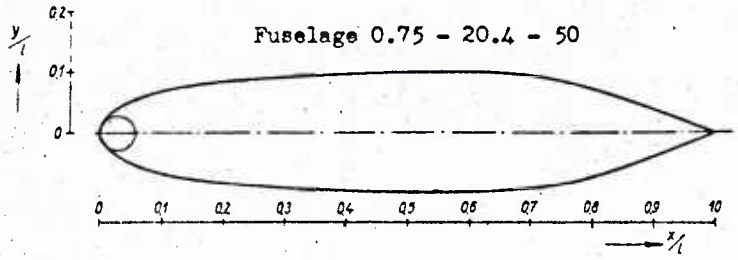

Pressure distribution

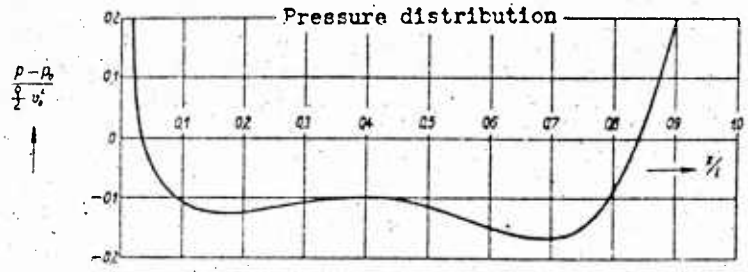

x/l	0	0.01	0.02	0.03	0.04	0.06	0.08	0.10	0.15	0.20	0.30	0.40	0.50	0.60	0.70	0.80	0.90	0.95	1.00
y/l	0	0.0224	0.0313	0.0367	0.0405	0.0455	0.0482	0.0489	0.0479	0.0453	0.0394	0.0329	0.0264	0.0199	0.0135	0.0075	0.0029	0.0009	0

$\frac{S}{l} = 2.75 \left(\frac{t_{max}}{l}\right)^2$

№ 10

Source-sink distribution

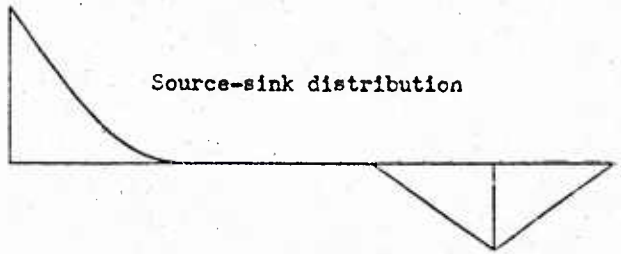

Fuselage 1.06 - 20.2 - 45

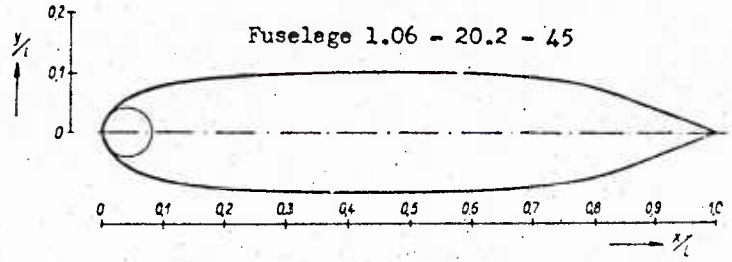

Pressure distribution

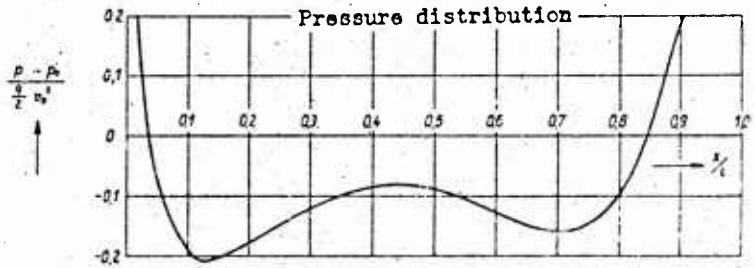

x/l	0	0.01	0.02	0.03	0.04	0.06	0.08	0.10	0.15	0.20	0.30	0.40	0.50	0.60	0.70	0.80	0.90	0.95	1.00
y/l	0	0.0325	0.0411	0.0461	0.0501	0.0560	0.0593	0.0599	0.0588	0.0558	0.0499	0.0434	0.0369	0.0304	0.0239	0.0178	0.0130	0.0109	0

$\frac{S}{l} = 1.06 \left(\frac{t_{max}}{l}\right)^2$

V_1

Source-sink distribution

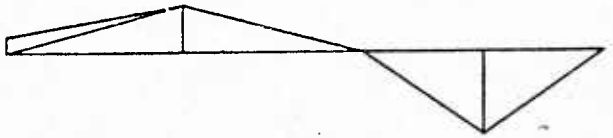

Fuselage 0.18 - 20 - 60

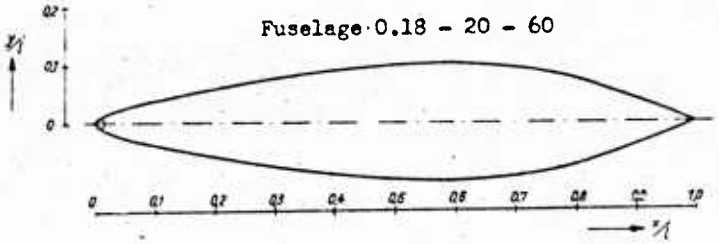

Pressure distribution

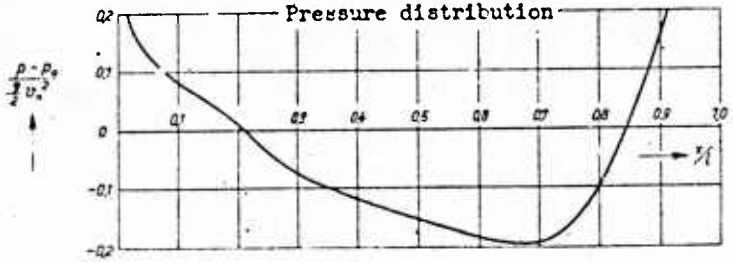

x_1	0	0,01	0,02	0,03	0,04	0,06	0,08	0,10	0,15	0,20	0,30	0,40	0,50	0,60	0,70	0,80	0,90	0,95	1,00
y_1	0	0,012	0,017	0,020	0,023	0,029	0,034	0,037	0,049	0,060	0,073	0,085	0,097	0,100	0,093	0,075	0,040	0,020	0

$$\frac{\rho}{l} = 0{,}16\,\frac{a^2_{max}}{l^2}$$

V_2

Source-sink distribution

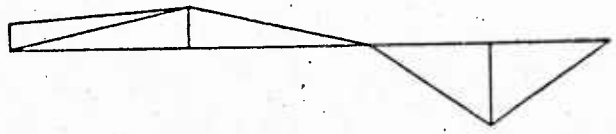

Fuselage 0.25 - 20 - 60

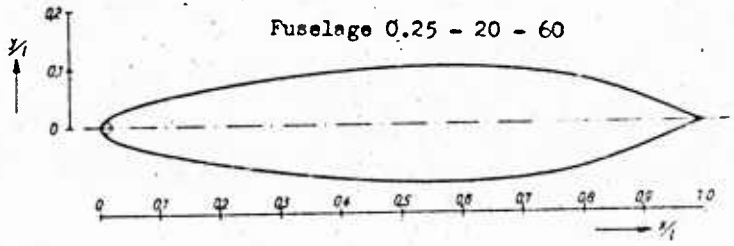

Pressure distribution

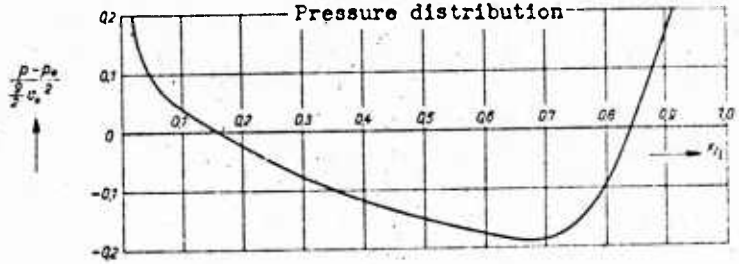

y_1/l	0	0,01	0,02	0,03	0,04	0,06	0,08	0,10	0,15	0,20	0,30	0,40	0,50	0,60	0,70	0,80	0,90	0,95	1,00
y_1/l	0	0,014	0,020	0,025	0,029	0,035	0,041	0,045	0,057	0,066	0,080	0,085	0,088	0,090	0,083	0,070	0,040	0,020	0

$$\frac{\rho}{l} = 0{,}25\,\frac{d^2_{max}}{l^2}$$

V3

Source-sink distribution

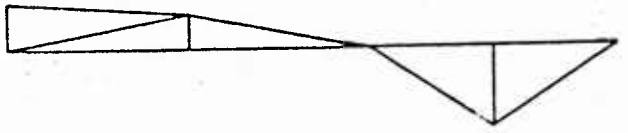

Fuselage 0.39 - 20 - 55

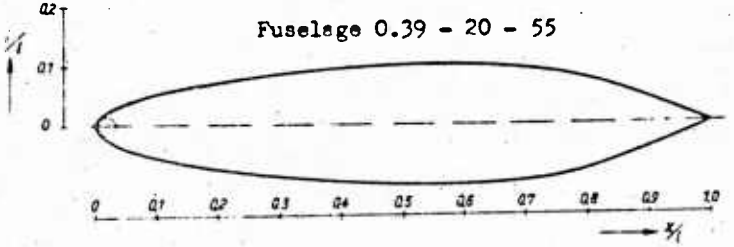

Pressure distribution

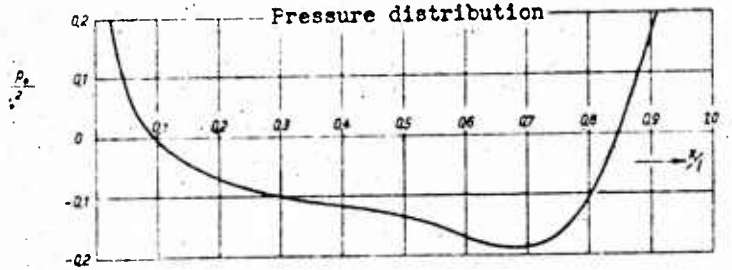

	0	0.01	0.02	0.03	0.04	0.05	0.06	0.10	0.15	0.20	0.30	0.40	0.50	0.60	0.70	0.80	0.90	0.95	1.00
	0	0.018	0.024	0.029	0.034	0.042	0.048	0.054	0.064	0.077	0.085	0.094	0.105	0.109	0.103	0.175	0.140	0.070	0

$\frac{f}{l} = 0.39 \frac{d_{max}}{l}$

V4

Source-sink distribution

Fuselage 0.38 - 20 - 50

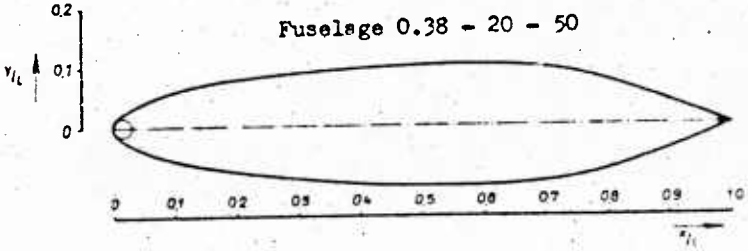

Pressure distribution

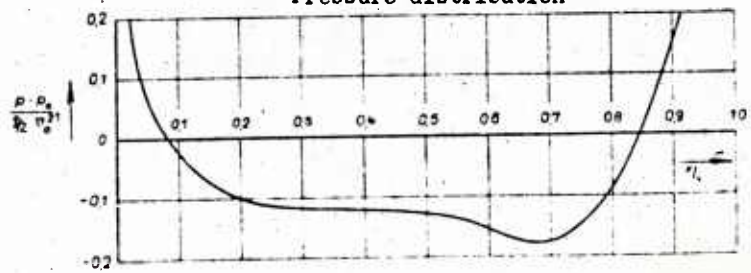

	0	0.01	0.02	0.03	0.04	0.06	0.08	0.10	0.15	0.20	0.30	0.40	0.50	0.60	0.70	0.80	0.90	0.95	1.00
	0	0.017	0.025	0.030	0.035	0.043	0.051	0.056	0.077	0.093	0.098	0.098	0.100	0.099	0.094	0.077	0.054	0.027	0

$\frac{f}{l} = 0.38 \frac{d_{max}}{l}$

V 5

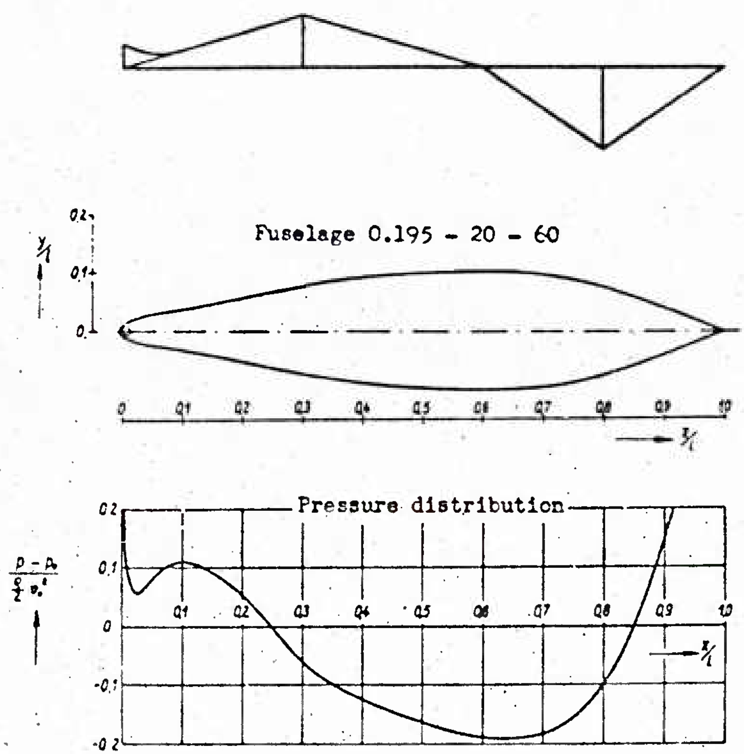

x/l	0	0.01	0.02	0.03	0.04	0.06	0.08	0.10	0.15	0.20	0.30	0.40	0.50	0.60	0.70	0.80	0.90	0.95	1.00
y/l	0	0.013	0.017	0.021	0.024	0.029	0.031	0.035	0.045	0.055	0.075	0.090	0.098	0.100	0.095	0.075	0.043	0.023	0

$\frac{q}{l} = 0.195 \frac{d^2_{max}}{l^2}$

V 6

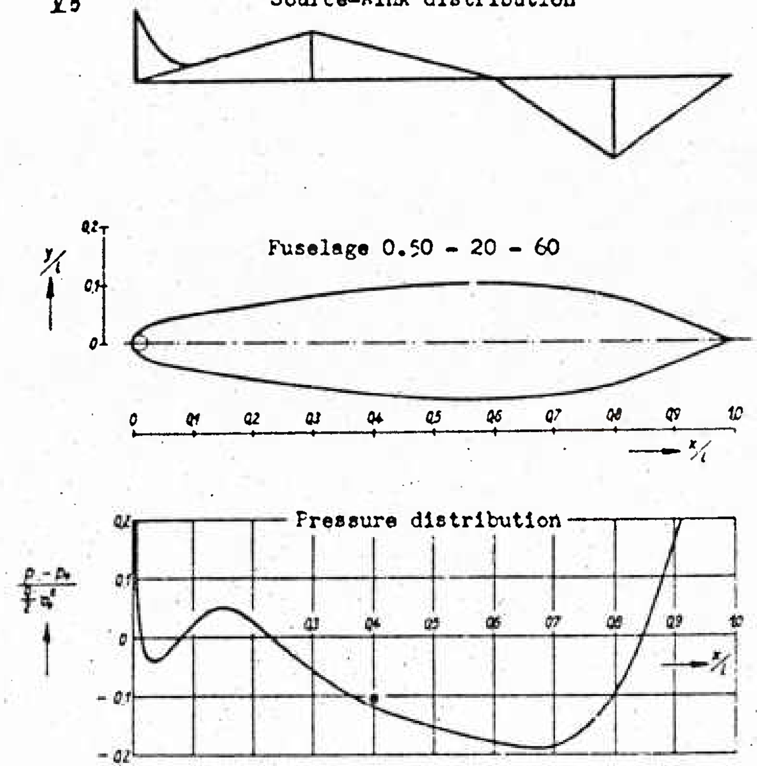

x/l	0	0.01	0.02	0.03	0.04	0.06	0.08	0.10	0.15	0.20	0.30	0.40	0.50	0.60	0.70	0.80	0.90	0.95	1.00
y/l	0	0.019	0.025	0.030	0.033	0.039	0.043	0.046	0.055	0.062	0.078	0.090	0.098	0.100	0.095	0.075	0.040	0.020	0

$\frac{q}{l} = 0.50 \frac{d^2_{max}}{l^2}$

V7

Source-sink distribution

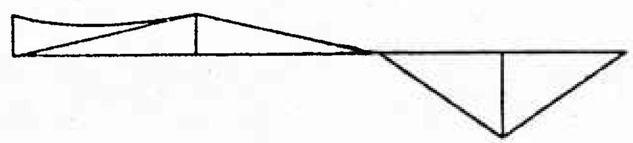

Fuselage 0.32 - 20 - 60

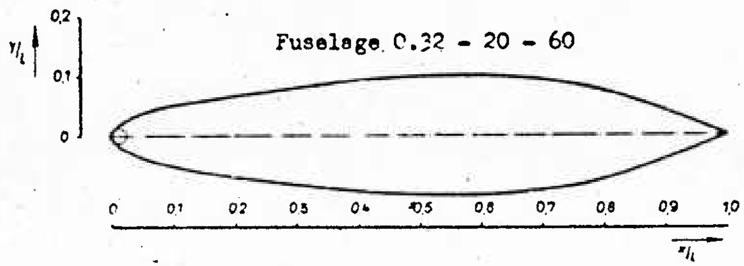

Pressure distribution

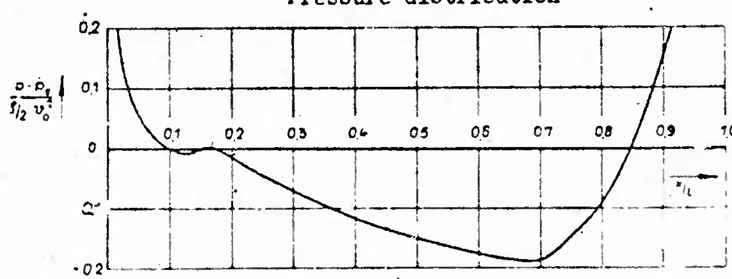

x/l	0	0.01	0.02	0.03	0.04	0.06	0.08	0.10	0.15	0.20	0.30	0.40	0.50	0.60	0.70	0.80	0.90	0.95	1.00
y/l	0	[illegible]	[illegible]	[illegible]	[illegible]	[illegible]	[illegible]	[illegible]	[illegible]	[illegible]	[illegible]	[illegible]	[illegible]	[illegible]	[illegible]	[illegible]	[illegible]	[illegible]	0

V8

Source-sink distribution

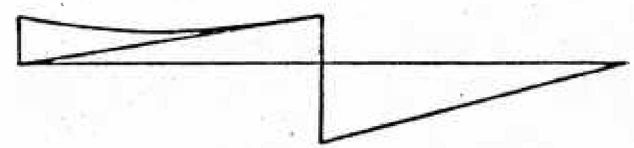

Fuselage 0.43 - 19.8 - 50

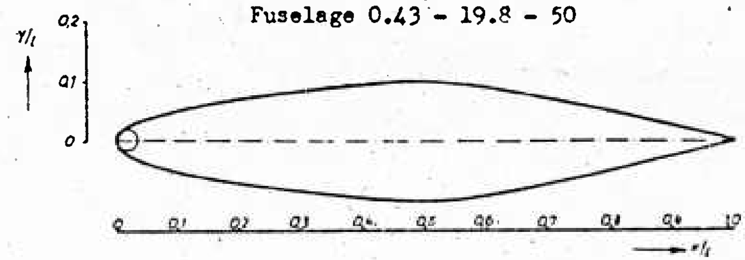

Pressure distribution

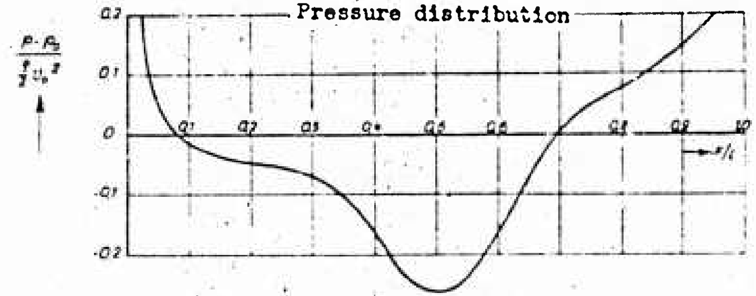

x/l	0	0,01	0,02	0,03	0,04	0,06	0,08	0,10	0,15	0,20	0,30	0,40	0,50	0,60	0,70	0,80	0,90	0,95	1,00
y/l	0	0,020	[illegible]	[illegible]	[illegible]	[illegible]	[illegible]	[illegible]	[illegible]	[illegible]	[illegible]	[illegible]	[illegible]	[illegible]	[illegible]	[illegible]	[illegible]	0,015	0

VI 1

Source-sink distribution

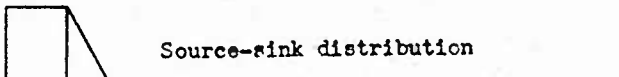

Fuselage 0.80 - 19.6 - 30

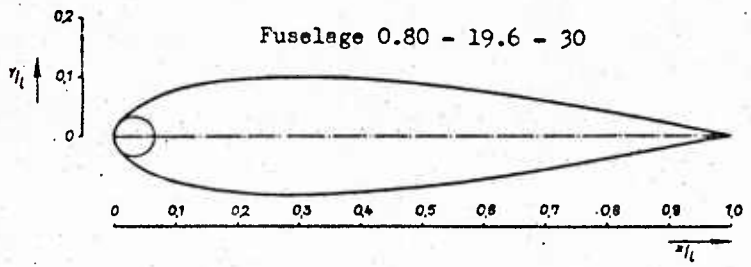

Pressure distribution

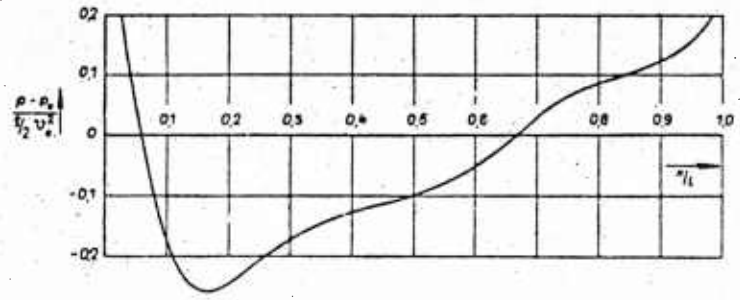

x/l	0	0,01	0,02	0,03	0,04	0,06	0,08	0,10	0,15	0,20	0,30	0,40	0,50	0,60	0,70	0,80	0,90	0,95	1,00
y/l	0	0,022	0,033	0,04	0,05	0,06	0,07	0,077	0,09	0,094	0,096	0,094	0,088	0,077	0,063	0,047	0,029	0,020	0

$\frac{1}{2} \cdot 0,80 \frac{d_{max}}{l}$

VI 2

Source-sink distribution

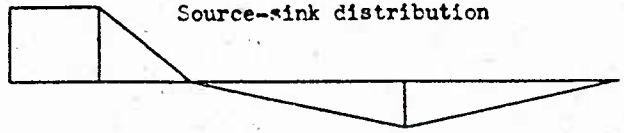

Fuselage 0.62 - 20 - 35

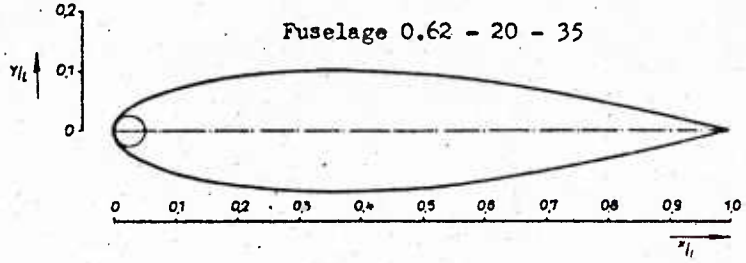

Pressure distribution

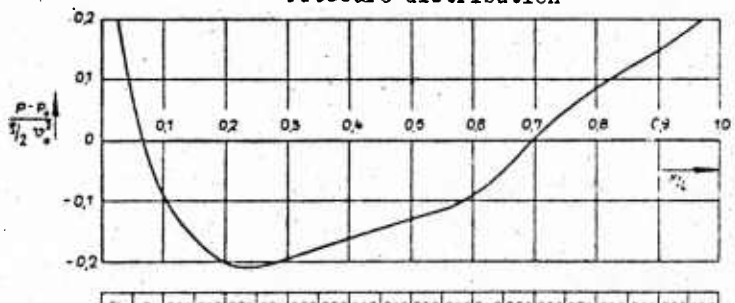

x/l	0	0,01	0,02	0,03	0,04	0,05	0,06	0,10	0,15	0,20	0,30	0,40	0,50	0,60	0,70	0,80	0,90	0,95	1,00
y/l	0	0,022	0,031	0,039	0,045	0,051	0,056	0,068	0,083	0,093	0,098	0,098	0,094	0,086	0,076	0,064	0,049	0,041	0

$\frac{1}{2} \cdot 0,62 \frac{d_{max}}{l}$

VI3

Source-sink distribution

Fuselage 0.40 - 20 - 50

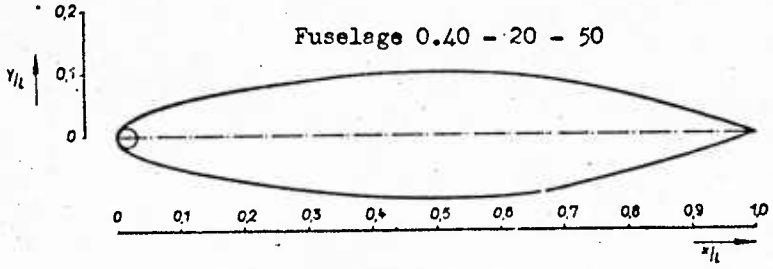

Pressure distribution

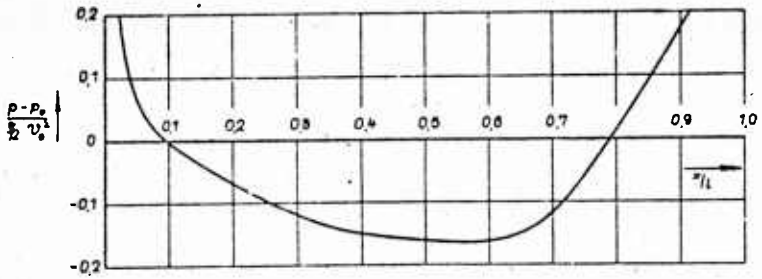

x/l	0	0,01	0,02	0,03	0,04	0,06	0,08	0,10	0,15	0,20	0,30	0,40	0,50	0,60	0,70	0,80	0,90	0,95	1,00
y/l	0	0,0018	0,0025	0,0030	0,0035	0,0042	0,0047	0,0055	0,0065	0,0074	0,0086	0,0096	0,0104	0,0107	0,0108	0,0105	0,0096	0,0087	0,0016	0

$\frac{1}{l}+0,40\ d'_{max}$

VI4

Source-sink distribution

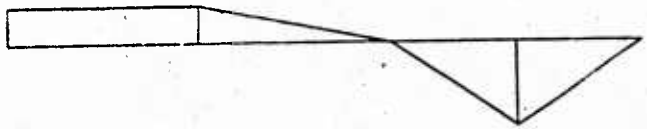

Fuselage 0.29 - 20 - 60

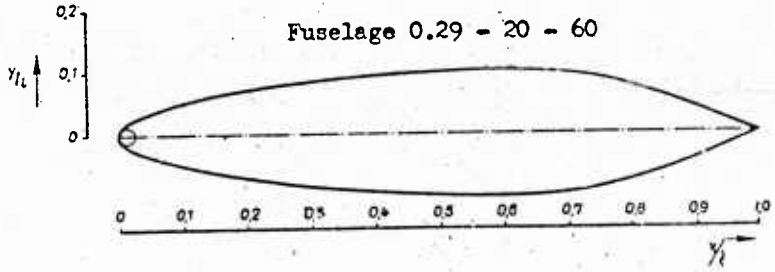

Pressure distribution

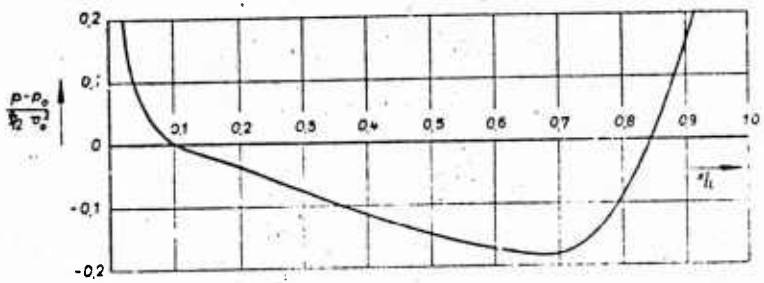

x/l	0	0,01	0,02	0,03	0,04	0,06	0,08	0,10	0,15	0,20	0,30	0,40	0,50	0,60	0,70	0,80	0,90	0,95	1,00
y/l	0	0,0015	0,0021	0,0025	0,0030	0,0038	0,0044	0,0049	0,0061	0,0073	0,0085	0,0092	0,0097	0,0100	0,0097	0,0091	0,0084	0,0077	0,0020	0

$\frac{1}{l}+0,29\ d'_{max}$

VI 5

Source-sink distribution

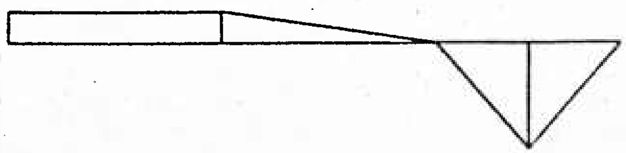

Fuselage 0.26 - 20 - 65

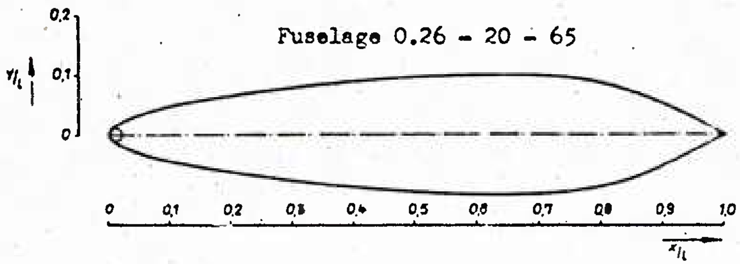

Pressure distribution

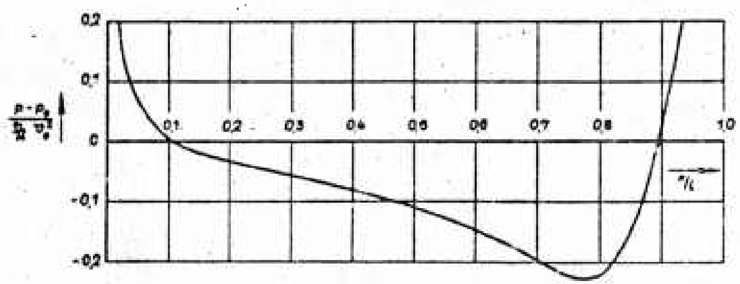

x/l	0	0,01	0,02	0,03	0,04	0,06	0,08	0,10	0,16	0,20	0,30	0,40	0,50	0,60	0,70	0,80	0,90	0,96	1,00
y/l	0	0,014	0,020	[illegible]	[illegible]	[illegible]	[illegible]	[illegible]	0,057	[illegible]	[illegible]	[illegible]	[illegible]	[illegible]	[illegible]	[illegible]	0,052	0,027	0

$f \cdot 0{,}26\,\frac{d'_{max}}{l}$

VI 6

Source-sink distribution

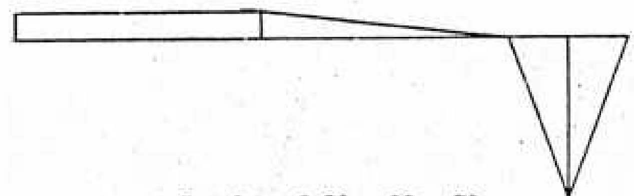

Fuselage 0.23 - 20 - 70

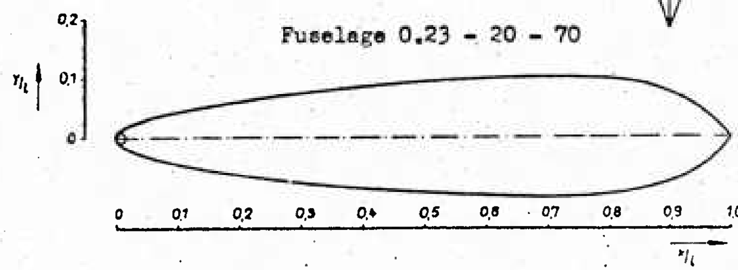

Pressure distribution

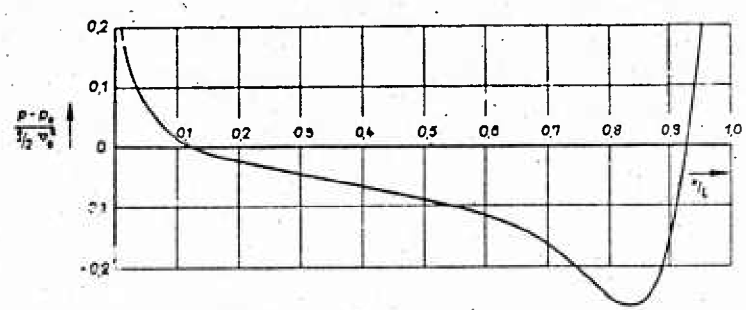

x/l	0	0,01	0,02	0,03	0,04	0,06	0,08	0,10	0,15	0,20	0,30	0,40	0,50	0,60	0,70	0,80	0,90	0,95	1,00
y/l	0	0,013	0,019	0,024	[illegible]	[illegible]	0,040	0,046	0,054	0,060	0,075	0,085	0,097	0,098	0,100	0,096	0,075	0,050	0

$f \cdot 0{,}23\,\frac{d'_{max}}{l}$

Source-sink distribution

VII 7

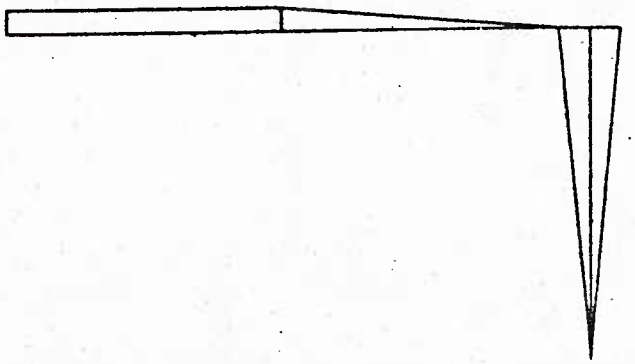

Fuselage 0.21 - 20 - 75

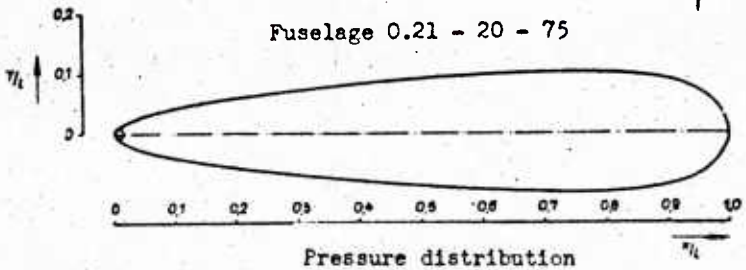

Pressure distribution

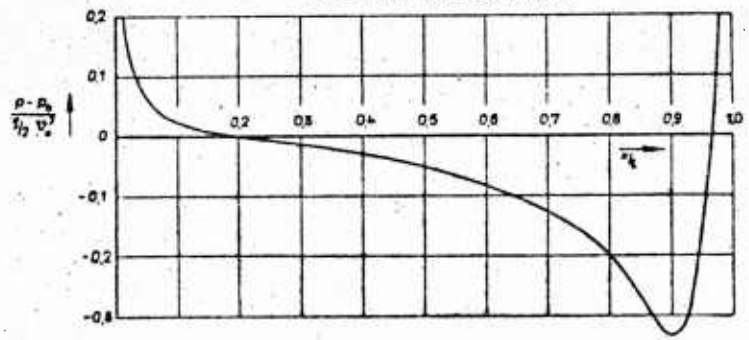

	0	0,01	0,02	0,04	0,06	0,08	0,10	0,15	0,20	0,30	0,40	0,50	0,60	0,70	0,80	0,90	0,96	1,00			
	0																				0

-0,21 $c_{p_{max}}$

VI 1 Source-sink distribution

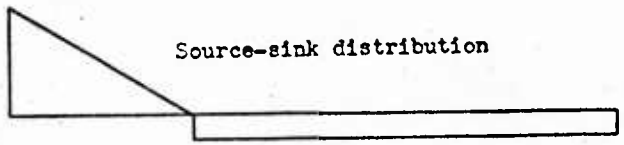

Fuselage 0.80 - 19.8 - 30

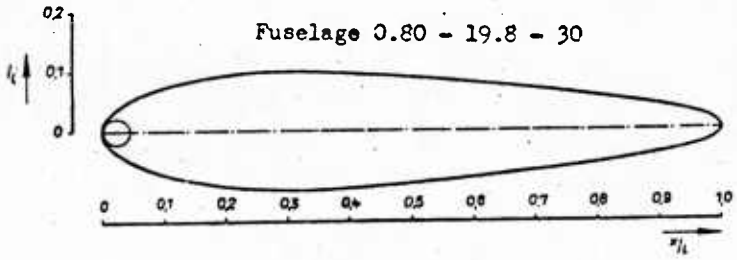

Pressure distribution

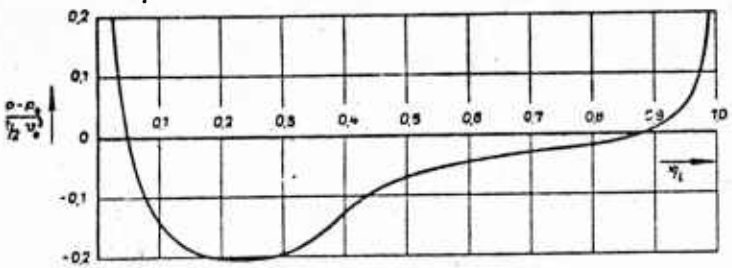

x/l	0	0,01	0,02	0,03	0,04	0,06	0,08	0,10	0,15	0,20	0,30	0,40	0,50	0,60	0,70	0,80	0,90	0,95	1,00
y/l	0	0,0025	0,0035	0,004	0,005	0,006	0,0065	0,007	0,0075	0,0084	0,0092	0,0098	0,0099	0,0096	0,0087	0,0072	0,0053	0,0037	0

$\frac{y}{l} = 0{,}80 \frac{d}{l}$

VI 2 Source-sink distribution

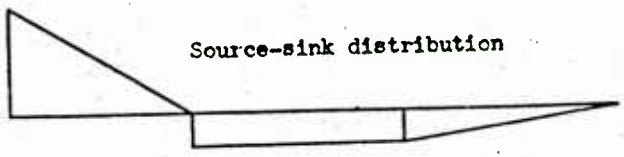

Fuselage 0.80 - 19.4 - 30

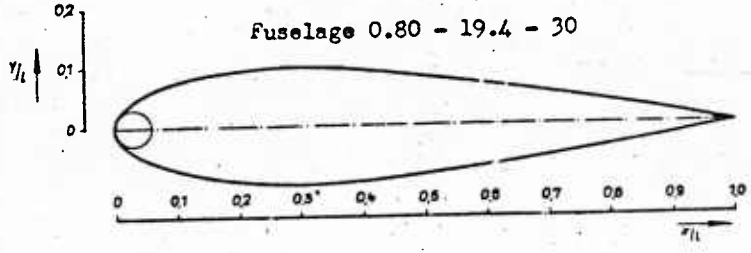

Pressure distribution

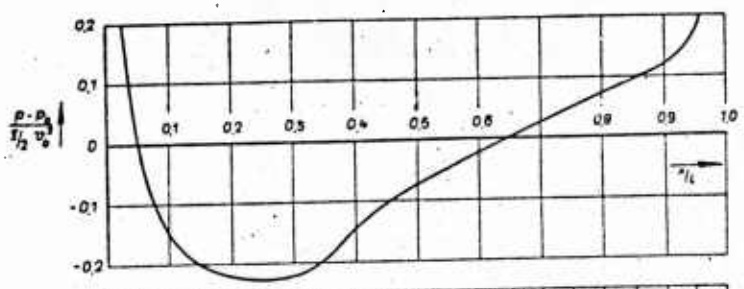

x/l	0	0,01	0,02	0,03	0,04	0,06	0,08	0,10	0,15	0,20	0,30	0,40	0,50	0,60	0,70	0,80	0,90	0,95	1,00
y/l	0	0,0025	0,0036	0,004	0,005	0,006	0,0065	0,007	0,0075	0,0084	0,009	0,0098	0,0097	0,0094	0,0085	0,0070	0,0051	0,0035	0

$\frac{y}{l} = 0{,}80 \frac{d}{l}$

VII 3

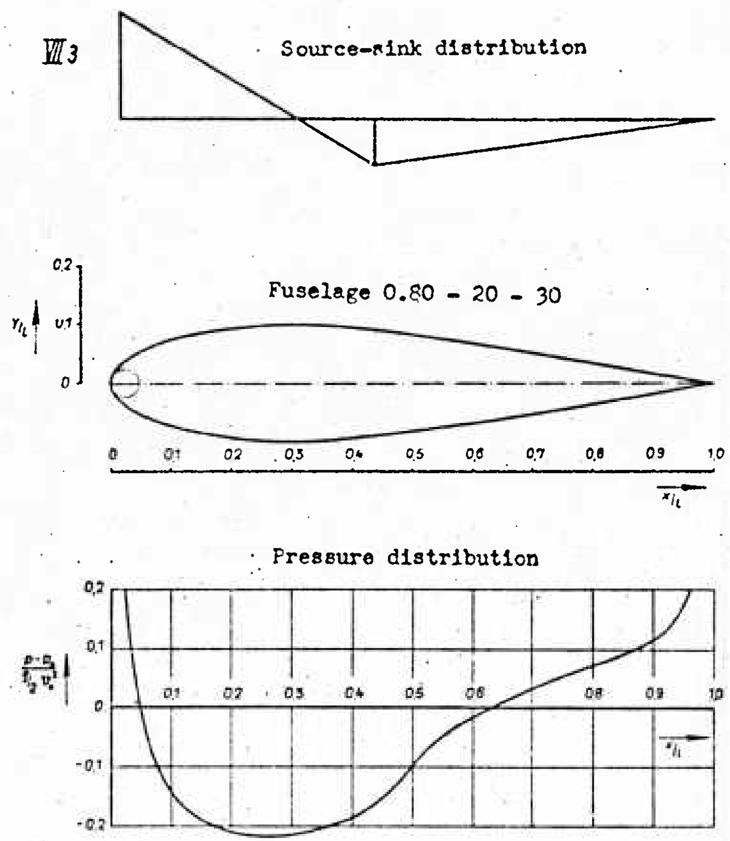

x/l	0	0.01	0.02	0.03	0.04	0.05	0.08	0.10	0.15	0.20	0.30	0.40	0.50	0.60	0.70	0.80	0.90	0.95	1.00
y/l	0	0.025	0.035	0.045	0.048	0.058	0.066	0.075	0.084	0.092	0.100	0.094	0.087	0.068	0.057	0.035	0.019	0.009	0

$\frac{y}{l} \cdot 0.80 \frac{d_{max}}{l}$

VII 4

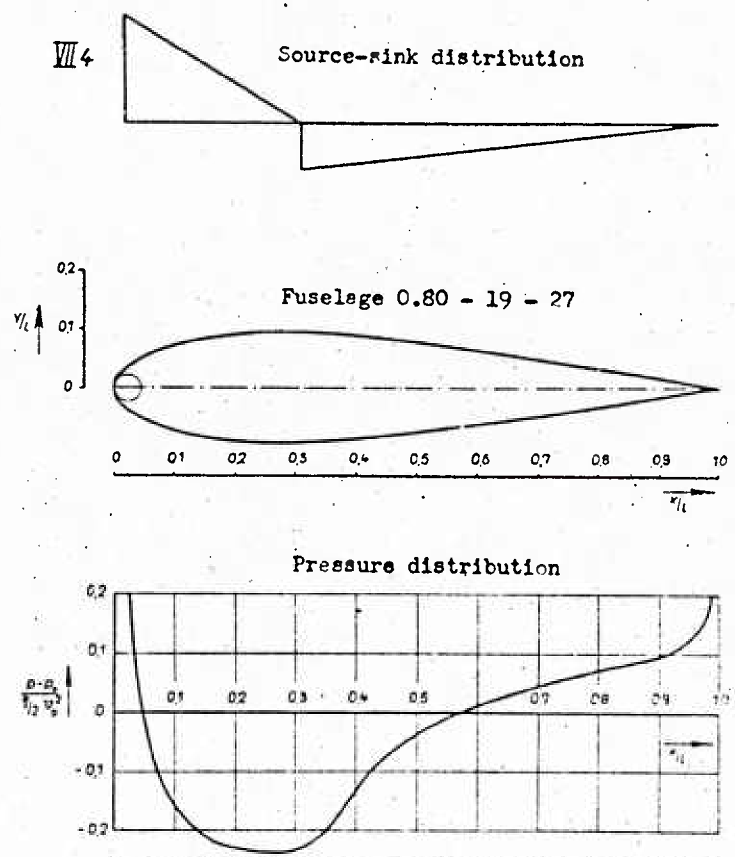

x/l	0	0.01	0.02	0.03	0.04	0.06	0.08	0.10	0.15	0.20	0.30	0.40	0.50	0.60	0.70	0.80	0.90	0.95	1.0
y/l	0	0.025	0.035	0.043	0.048	0.058	0.066	0.075	0.084	0.090	0.094	0.088	0.076	0.064	0.048	0.032	0.016	0.008	0

$\frac{y}{l} \cdot 0.80 \frac{d_{max}}{l^2}$

VIII 1

Source-sink distribution

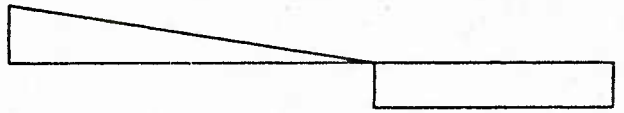

Fuselage 0.45 - 20 - 50

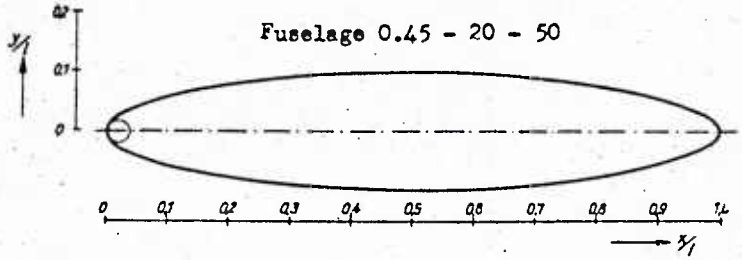

Pressure distribution

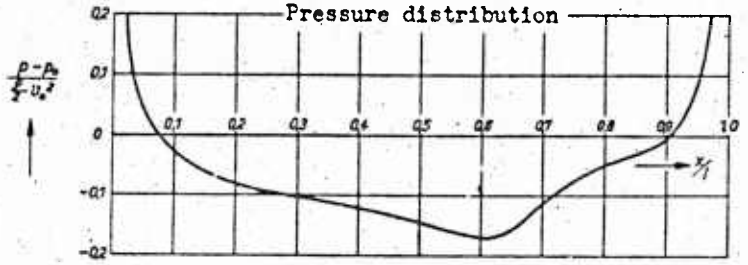

x/l	0	0,01	0,02	0,03	0,04	0,06	0,08	0,10	0,15	0,20	0,30	0,40	0,50	0,60	0,70	0,80	0,90	0,95	0,97	0,98	0,99	1,00
y/l	0	0,0270	0,0377	0,0433	0,0477	0,0545	0,0592	0,0628	0,0684	0,0716	0,0749	0,0757	0,0700	0,0606	0,0490	0,0370	0,0253	0,0197	0,0174	0,0154	0,0135	0

$\frac{\varrho}{l} = 0{,}45\,\frac{d^2_{max}}{l^2}$

VIII 2

Source-sink distribution

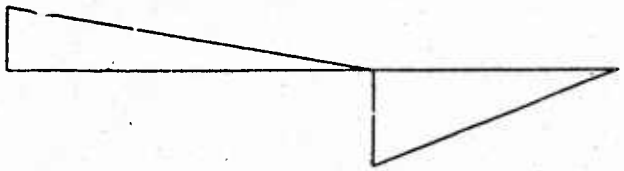

Fuselage 0.49 - 20.8 - 50

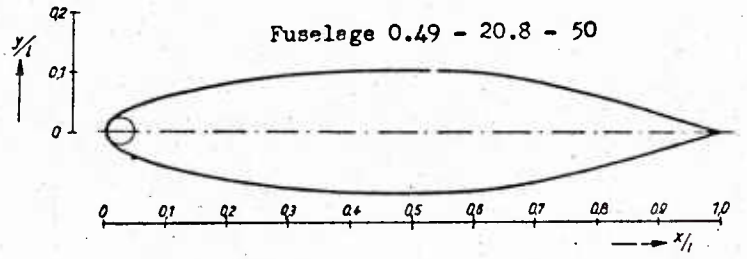

Pressure distribution

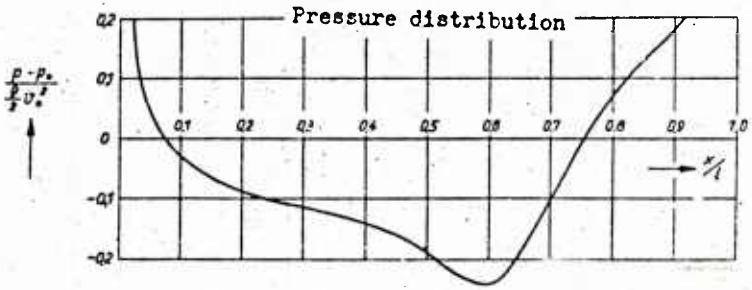

x/l	0	0,01	0,02	0,03	0,04	0,06	0,08	0,10	0,15	0,20	0,30	0,40	0,50	0,60	0,70	0,80	0,90	0,95	1,00
y/l	0	0,0225	0,0321	0,0385	0,0417	0,0449	0,0458	0,0461	0,0473	0,0467	0,0394	0,0301	0,0204	0,0140	0,0100	0,0083	0,0057	0,0038	0,0015	0

$\frac{\varrho}{l} = 0{,}49\,\frac{d^2_{max}}{l^2}$

VIII 3

Source-sink distribution

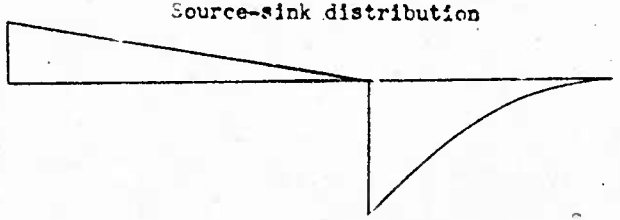

Fuselage 0.48 - 20 - 50

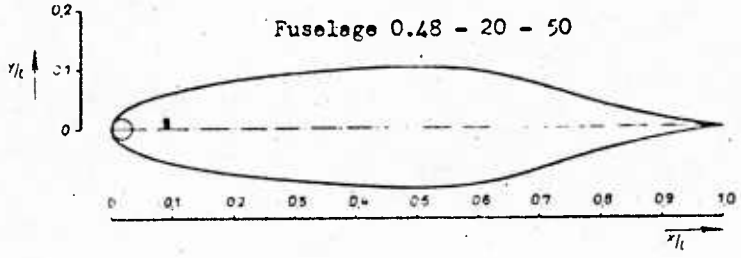

Pressure distribution

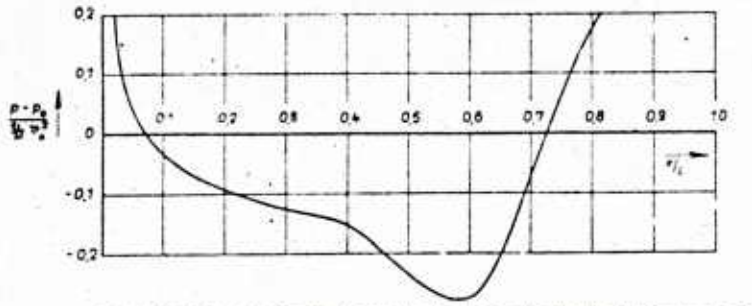

x/l	0	001	002	003	004	006	008	010	015	020	030	040	050	060	070	080	085	090	095	100
y/l	0	0022	0028	0035	0038	0043	0047	0051	0059	0070	0078	0085	0090	0096	0100	0094	0072	0043	0027	0017	0006	0

$\frac{1}{l^2} \cdot 0{,}48\, d^2_{max}$

VIII 4

Source-sink distribution

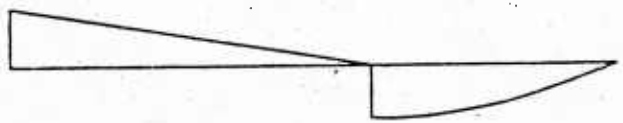

Fuselage 0.45 - 20 - 50

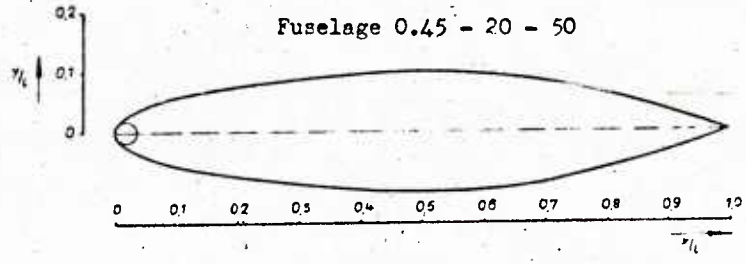

Pressure distribution

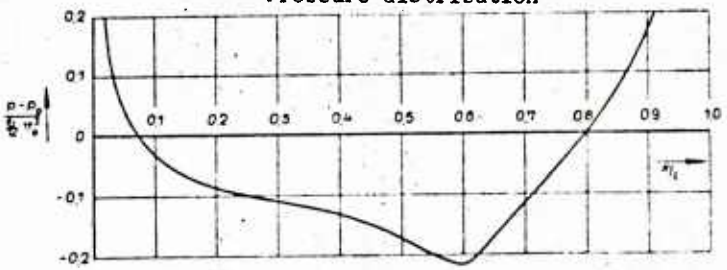

x/l	0	001	002	005	004	006	008	010	015	020	030	040	050	060	070	080	090	095	100
y/l	0	0019	0027	0035	0043	0049	0053	0057	0066	0076	0086	0094	0096	0101	0097	0084	0067	0035	0017	0

$\frac{1}{l^2} \cdot 0{,}45\, d^2_{max}$

VII 5

Source-sink distribution

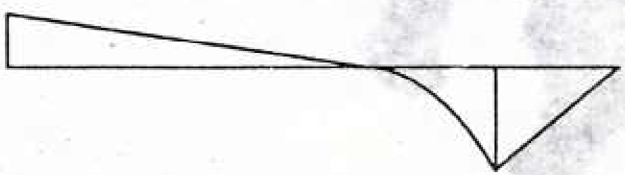

Fuselage 0.39 - 20 - 60

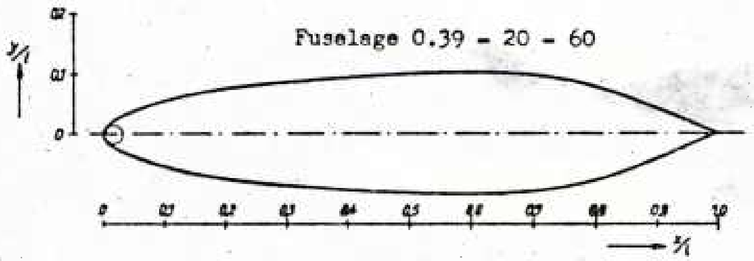

Pressure distribution

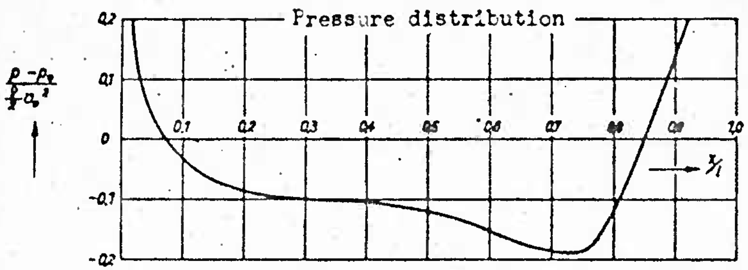

x/l	0	[illegible]	[illegible]	0,03	0,04	[illegible]	[illegible]	[illegible]	[illegible]	[illegible]	[illegible]	[illegible]	[illegible]	[illegible]	[illegible]	[illegible]	[illegible]	[illegible]	[illegible]
y/l	0	[illegible]	[illegible]	[illegible]	[illegible]	[illegible]	[illegible]	[illegible]	[illegible]	[illegible]	[illegible]	[illegible]	[illegible]	[illegible]	[illegible]	[illegible]	[illegible]	[illegible]	0

$\frac{f}{l} = 0{,}39 \frac{d^2_{max}}{l^2}$

VII 6

Source-sink distribution

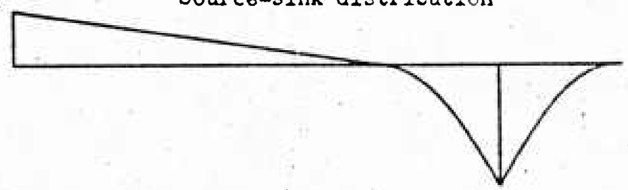

Fuselage 0.39 - 20 - 60

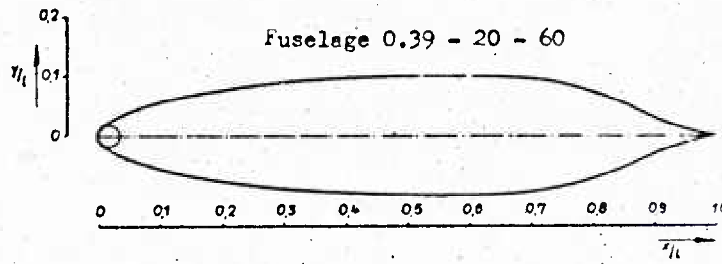

Pressure distribution

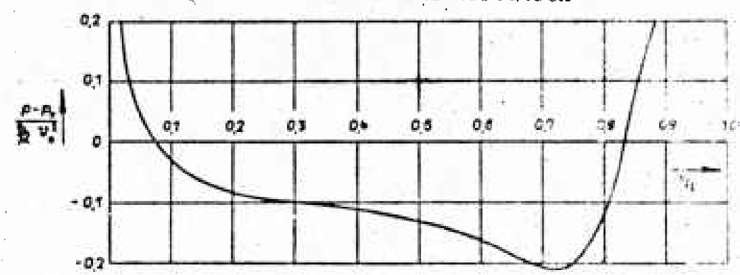

x/l	0	0,01	0,02	0,03	0,04	0,06	0,08	0,10	0,15	0,20	0,30	0,40	0,50	0,60	0,70	0,80	0,85	0,90	0,95	1,00
y/l	0	0,017	0,024	0,030	0,035	0,043	0,050	0,055	0,067	0,075	0,089	0,095	0,098	0,100	0,095	0,075	0,064	0,037	[illegible]	[illegible]

$\frac{f}{l} = 0{,}38 \frac{d^2_{max}}{l^2}$

VII 7

Source-sink distribution

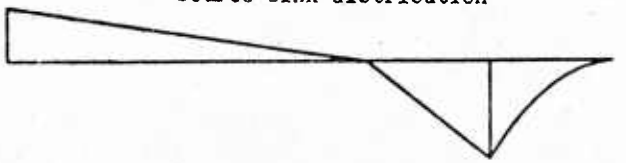

Fuselage 0.39 - 20 - 55

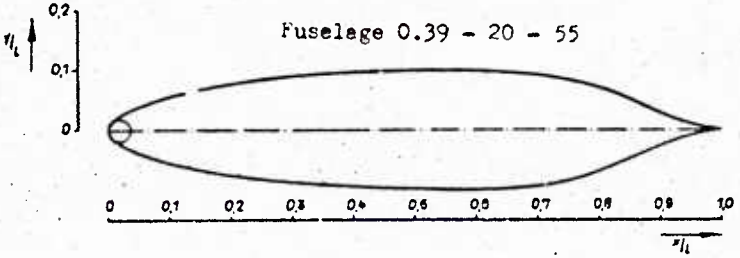

Pressure distribution

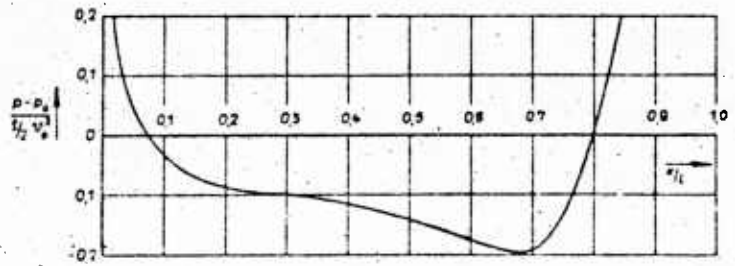

x/l	0	0,01	0,02	0,03	0,04	0,05	0,06	0,08	0,10	0,15	0,20	0,30	0,40	0,50	0,60	0,70	0,80	0,85	0,90	0,95	1,00
y/l	0																				0

$+0{,}39\ \frac{d\,l_{max}}{l}$

VII 8

Source-sink distribution

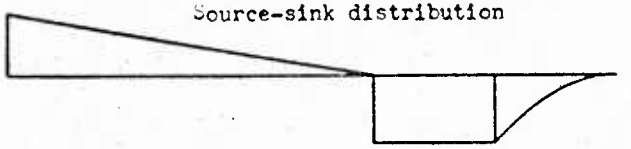

Fuselage 0.48 - 20.6 - 50

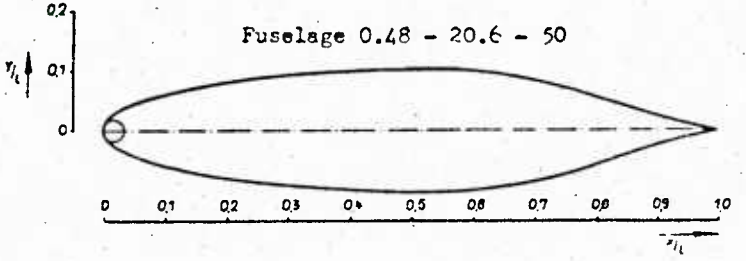

Pressure distribution

x/l	0	0,01	0,02	0,03	0,04	0,06	0,08	0,10	0,15	0,20	0,30	0,40	0,50	0,60	0,70	0,80	0,85	0,90	0,95	1,00
y/l	0																			0

$+0{,}48\ \frac{d\,l_{max}}{l}$

TITLE: Pressure Distributions over Bodies of Revolution for Axial Flow 006800

AUTHOR(S): Brand, M.

ORIGINATING AGENCY: Aerodynamische Versuchsanstalt, Goettingen, E.V.

PUBLISHED BY: Zentrale fuer wissenschaftliches Berichtswesen, Berlin-Adlershof

ATI- 42556 *

REVISION (None)

ORIG. AGENCY NO. (None)

PUBLISHING AGENCY NO. UM-3206

U

DATE	DOC. CLASS.	COUNTRY	LANGUAGE	PAGES	ILLUSTRATIONS
Dec '44	Unclass.	Germany	German	49	tables, diagrs, graphs

FOREIGN TITLE: Druckverteilungen von Rotationskoerpern. . .Anstroemung

TRANSLATION BY: Navy Department, David Taylor Model Basin, Washington, D.C. April '47

ABSTRACT: P2014 Pressure Distribution in Bodies of Revolution

Calculated pressure distributions are given for 12 half-bodies and for 59 bodies of revolution for the case of axial flow. The nose radius, the thickness distribution, and the trailing-edge angle were varied, while the fineness ratio was assumed practically constant throughout at 1:5. After a review of the systematic calculations, examples are given for bodies with assigned contours, as well as a discussion of the effects of other fineness ratios on the pressure distribution.

NOTE: Previously cataloged as Captured Document No. ZWB/UM/Re 3206

~~DISTRIBUTION: Copies of this report obtainable from Central Air Documents Office; Attn: MCIDXD~~

DIVISION: Aerodynamics (2)

SECTION: Aerodynamic Loads (8)

SUBJECT HEADINGS: Load distribution - Thickness ratio effect (55780); Bodies of revolution - Aerodynamics (16600)

AD-A800 396

TECHNICAL INDEX

Wright-Patterson Air Force Base
Dayton, Ohio

NTIS, Auth.: USNSRDC 19, 16 Apr 74